Nano Research

Open Access

Review Article

Single-molecule spin devices: Fundamentals, advances, and prospects

Yuzhe Zhang[1,§], Wei Si[1,§], Xukui Hou[1], Qinghua Gao[1], Cong Zhao[1], Ruizhi Liang[1], Jie Guo[1] ✉, Mingliang Li[2,3] ✉, Chuancheng Jia[1] ✉, and Xuefeng Guo[1,4] ✉

[1] *Center of Single-Molecule Sciences, Institute of Modern Optics, Frontiers Science Center for New Organic Matter, Tianjin Key Laboratory of Micro-Scale Optical Information Science and Technology, College of Electronic Information and Optical Engineering, Nankai University, Tianjin 300350, China*
[2] *Department of Chemistry, The University of Hong Kong, Hong Kong 999077, China*
[3] *School of Materials Science and Engineering, Beijing Institute of Technology, Beijing 100081, China*
[4] *Beijing National Laboratory for Molecular Sciences, National Biomedical Imaging Center, College of Chemistry and Molecular Engineering, Peking University, Beijing 100871, China*
§ *Yuzhe Zhang and Wei Si contributed equally to this work.*

Cite this article: *Nano Research*, **2026**, *19*, 94908552. https://doi.org/10.26599/NR.2026.94908552

ABSTRACT: Single-molecule spintronics is an emerging interdisciplinary field that integrates molecular electronics with spin-based information science, offering novel pathways for encoding, manipulating, and detecting spin at the molecular level. This review explores the fundamental principles, advances, and prospects of single-molecule spin devices, emphasizing the manipulation of spin states in various molecular systems, such as single-molecule magnets, spin crossover complexes, organic radicals, and chiral molecules. Due to their intrinsic quantum characteristics and tunable functionalities, these systems serve as ideal platforms for investigating spin-related phenomena including Kondo effects, spin filtering, and thermoelectric effects. The integration of molecular junctions with advanced measurement techniques, such as spin-polarized scanning tunneling microscopy and electron spin resonance, has significantly advanced the understanding of spin transport and coherence in single-molecule configurations. Furthermore, potential applications of these molecules in devices like spin valves, spin switches, and quantum bits are discussed, highlighting their promise for realizing low-power and high-efficiency spintronic technologies. Despite significant progress, several challenges remain in terms of stability, reproducibility, and scalability, necessitating further research into molecular design, interfacial engineering, and quantum coherence to enable practical applications in molecular spintronics and quantum information science.

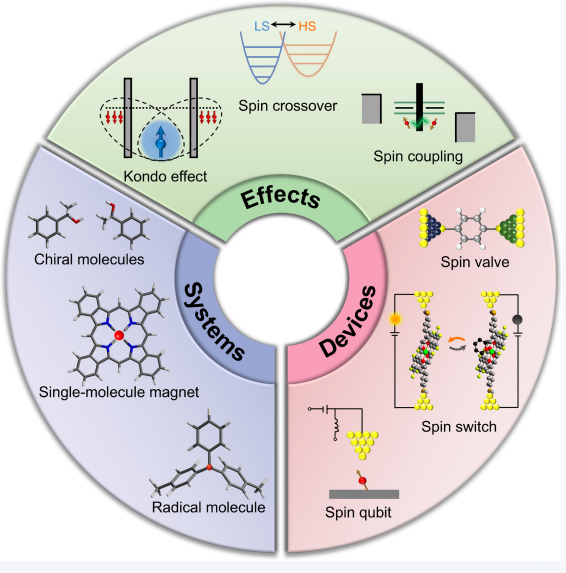

KEYWORDS: single-molecule spintronics, electron spin, spin effect, molecular spin device, spin qubit

1 Introduction

Single-molecule spintronics represents an interdisciplinary frontier bridging molecular electronics and spin-based information science, devoted to the encoding, manipulation, and detection of spin degrees of freedom at the single-molecule level [1, 2]. By integrating the structural precision of chemistry with the functional insights of condensed-matter physics, this field aims to develop a new generation of devices where spin, rather than charge, serves as the primary information carrier [3]. Molecular systems provide an ideal platform for such investigations due to their unique quantum characteristics. They constitute well-defined quantum systems in which geometry, orbital symmetry, and chemical bonding can be systematically tailored [4]. In addition, their small capacitance, tunable energy levels, and versatile coupling to electric, magnetic, optical, and thermal fields enable operations with low

Received: January 1, 2026; **Revised:** February 8, 2026
Accepted: February 10, 2026

✉Address correspondence to Xuefeng Guo, guoxf@pku.edu.cn; Chuancheng Jia, jiacc@nankai.edu.cn; Mingliang Li, liml@bit.edu.cn; Jie Guo, gj@nankai.edu.cn

energy consumption while maintaining controllable quantum responses [5].

Despite rapid progress, realizing the robust and controllable spin behavior at the single-molecule scale remains a fundamental challenge. Spin states are highly sensitive to the interplay among exchange interactions, spin-orbit coupling, electron–phonon coupling, and molecule–electrode hybridization [6]. Variations in contact geometry and molecular conformation pose additional challenges to the reproducibility, while thermal fluctuations and environmental noise accelerate spin relaxation and decoherence [7]. Consequently, a deep understanding of how these microscopic interactions govern macroscopic spin-based functionalities is essential for designing reliable spintronic devices at the molecular scale.

To address these challenges, a variety of molecular platforms have been developed to investigate and harness spin phenomena [8]. Single-molecule magnets (SMMs) based on transition-metal or lanthanide (Ln) ions exhibit large magnetic anisotropy and slow spin relaxation, making them representative systems for nonvolatile molecular memory [9]. Spin crossover (SCO) complexes exhibit reversible transitions between high-spin (HS) and low-spin (LS) states in response to external stimuli such as temperature [10–12], pressure [13], light [14], or bias voltage [15], offering a molecular model for switchable magnetic behaviors. Open-shell organic radicals provide stable spin-1/2 centers characterized by long coherence time and flexible chemical tunability [16]. Meanwhile, chiral molecules introduce spin selectivity through their intrinsic symmetry breaking, enabling spin filtering in the absence of magnetic order [17, 18]. Collectively, these systems establish a versatile chemical foundation for studying spin interactions, coherence, and relaxation at the molecular scale.

Advances in experimental spectroscopies and measurement methodologies have yielded deeper insights into the spin behavior of these molecular systems [19, 20]. The introduction of a gate electrode has been particularly transformative, enabling precise tuning of molecular junctions to activate their intrinsic self-regulating capabilities. This synergy reveals effects such as self-controlled coupling for resonant transport, self-controlled filtering based on spin and energy, and self-controlled thermoelectric conversion, highlighting how external fields can harness built-in molecular functionalities. Furthermore, the application of thermal gradients across molecular junctions has uncovered spin-dependent thermoelectric effects, directly linking spin transport to energy conversion [21]. These electrical methods are powerfully complemented by spectroscopic techniques. Electron spin resonance (ESR) integrated with transport measurements enables the coherent manipulation of single spins, while optically detected magnetic resonance and ultrafast pump-probe spectroscopy extend the detection into the temporal domain, quantifying spin dynamics and coherence [22]. Realizing such measurements relies on robust single-molecule junctions. Techniques such as mechanically controllable break junction (MCBJ), electromigrated nanogaps, and scanning probe microscopy form the foundational platforms for creating stable molecular bridges between metallic electrodes [23]. MCBJ enables precise regulation of the molecular junction gap, thereby facilitating the formation of single-molecule contacts and supporting nanoscale electrical measurements. In contrast, electromigrated nanogaps are formed through the controlled electrical breakdown of metallic wires, creating reproducible nanometer-scale gaps with molecular-level precision. Scanning probe microscopy, particularly scanning tunneling microscopy (STM), provides atomic-resolution imaging and direct probing of molecular electronic states, making it an indispensable tool for investigating spin and electronic transport properties in single-molecule junctions. Concurrently, the development of two-dimensional electrodes with molecularly defined van der Waals gaps has improved the stability and reproducibility, providing the low-noise and spin-transparent interfaces essential for reliable data acquisition [24].

This review follows a systematic framework that progresses from fundamental spin-bearing molecular systems to representative spin-related effects and finally to device-level realizations. By correlating molecular structures, interfacial coupling, and quantum transport mechanisms, we aim to clarify how spin states emerge, evolve, and are harnessed in single-molecule junctions. Through this arrangement, this review seeks to provide both a conceptual overview of the field and a roadmap for developing future molecular-scale spintronic and quantum information devices.

2 Single-molecule spin systems

Single-molecule spin systems epitomize the convergence of molecular design and quantum phenomena, offering a versatile platform to encode, manipulate, and transport information through electron spin. The fundamental challenge in this field extends beyond mere spin detection to precise engineering of spin states and their dynamics for technological applications. This pursuit has given rise to distinct yet complementary molecular archetypes, each tailored to address a specific aspect of spin control. For instance, the quest for persistent spin states, essential for memory and qubit applications, finds its molecular embodiment in SMMs, where synthetic efforts aim to tailor the energy landscape so as to maximize the barrier against magnetization relaxation. In a complementary manner, SCO compounds exemplify the dynamic spin state bistability, undergoing reversible transitions between HS and LS configurations in response to external stimuli, thereby functioning as intrinsic molecular switches. To interface these molecular spin units with the external world, the challenge of generating spin-polarized currents is elegantly solved by chiral molecules via the chiral-induced spin selectivity (CISS) effect, which leverages structural asymmetry to function as highly efficient and non-magnetic spin filters. Meanwhile, organic radical molecules, with their inherent and stable unpaired electrons, serve as ideal conduits and probes for investigating spin transport and many-body correlations directly within single-molecule junctions. Collectively, these systems form a coherent research paradigm, ranging from stable spin memory to spin state switching, and to the generation and transmission of spin information, thereby addressing the core challenges of scalability, coherence, and integration in molecular spintronics and quantum information science.

2.1 Single-molecule magnets

SMMs are commonly organized into mononuclear, dinuclear, and polynuclear families based on the use of either 3d transition metals or 4f Ln. Complexes composed solely of 3d ions often exhibit the limited performance due to their relatively weak spin-orbit coupling, which leads to small magnetic anisotropy, rapid magnetic relaxation, and consequently a low blocking temperature (T_B). In contrast, Ln-based SMMs exploit strong spin-orbit coupling and

large ionic radii to generate pronounced axial crystal fields and robust anisotropy barriers. Ions, such as Tb^{III}, Dy^{III}, and Er^{III}, retain substantial orbital angular momentum, making them particularly effective in this context. A canonical case is Tb-phthalocyanine ($TbPc_2$, Fig. 1(a)), where a Tb^{III} center is sandwiched between two Pc ligands that impose a high-symmetry coordination field. This geometry stabilizes the axial magnetic moment, enhances the effective energy barrier against magnetization reversal, and establishes $TbPc_2$ as a foundational model for the design and benchmarking of Ln SMMs. These observations motivate a design strategy focused on engineering the local crystal field to align the easy axis, maximize uniaxiality, and suppress fast relaxation pathways, such as quantum tunneling, direct processes, Raman processes, and Orbach processes, with the ultimate goal of increasing the effective barrier U_{eff} and raising T_B [25].

Beyond mononuclear species, dinuclear architectures employ bridging ligands to mediate magnetic exchange between two metal centers. In homometallic dimers (Fig. 1(b)), radical bridges can generate strong exchange interactions that lift the degeneracy of opposite projections of the ground state, thereby suppressing quantum tunneling of magnetization, which is a dominant mechanism for memory loss at low temperatures [26]. Heterometallic dimers (Fig. 1(c)), such as those combining a magnetic Ln ion with a diamagnetic Zn^{II} center, allow relatively independent tuning of the local crystal field at the Ln site and the exchange pathway through the bridge. This decoupled control provides a practical route to enlarge magnetic hysteresis while optimizing coercivity and remanence [27]. Extending further to polynuclear systems expands the chemical space for cooperative effects. Trinuclear heterometallic clusters such as Co_2Ln (Fig. 1(d)) exemplify the strategy, often placing the Ln in an O_8 square antiprismatic environment designed to maximize the axiality. However, increased structural complexity can also introduce new relaxation channels, including intermolecular interactions mediated by hydrogen-bonding networks that may inadvertently accelerate quantum tunneling, thereby highlighting the need for precise control over supramolecular packing [24]. Importantly, the polynuclear approach has enabled the robust SMM behavior in 3d-metal systems that are otherwise challenging to design. The Fe_4 cluster (Fig. 1(e)) demonstrates this capability: Strong super exchange among four HS Fe^{III} centers isolates a ground state ($S = 5$) with a substantial anisotropy barrier. Moreover, these molecules can self-assemble into ordered monolayers on conductive substrates such as gold, facilitating device integration [28]. The transition from bulk characterization to surface-supported studies is therefore crucial for technological relevance. STM combined with inelastic electron tunneling spectroscopy (IETS) provides single-molecule resolution of spin excitations and exchange constants. For instance, in Fe_4H on graphene/Ir(111) (Fig. 1(f)), these measurements reveal exchange parameters nearly identical to bulk values and show clear field-dependent Zeeman shifts, indicating minimal substrate perturbation. The joint evidence of robust hysteresis observed in surface-supported Fe_4 and spectroscopic confirmation of intact magnetic states in Fe_4H builds a coherent case that SMMs can retain their defining properties on surfaces and effectively bridges molecular design principles with practical implementation in quantum information and molecular spintronic platforms [29].

2.2 Spin crossover compounds

SCO compounds are coordination complexes that undergo reversible transitions between HS and LS states in response to external stimuli such as temperature, pressure, light, mechanical stress, or electric fields. First identified in Fe^{III} dithiocarbamate complexes and subsequently in Fe^{II} systems, SCO manifests most prominently as changes in magnetic susceptibility, elastic moduli, optical absorption, and even refractive index. These effects establish a direct connection between the electronic configuration of individual coordination centers and collective bulk properties. Thermodynamically, the LS state is typically enthalpically favored, while the HS state benefits from higher spin and vibrational

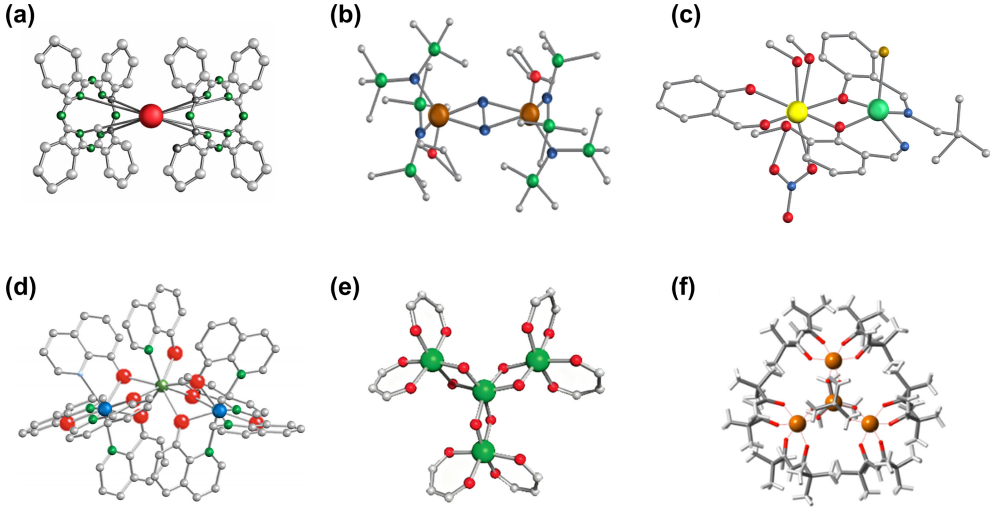

Figure 1 Molecular architectures of SMMs. (a) Mononuclear $TbPc_2$, exemplifying high axial symmetry and strong magnetic anisotropy. Reproduced with permission from Ref. [25], © WILEY-VCH Verlag GmbH & Co. KGaA, Weinheim 2017. (b) A radical-bridged homometallic dimer designed for enhanced exchange coupling to suppress quantum tunneling. Reproduced with permission from Ref. [26], © Springer Nature Limited 2011. (c) A heterometallic Ln-Zn dimer, allowing independent optimization of crystal field and exchange pathways. Reproduced with permission from Ref. [27], © WILEY-VCH Verlag GmbH & Co. KGaA, Weinheim 2011. (d) A trinuclear Co_2Ln cluster tailored for a highly axial square antiprismatic coordination geometry. Reproduced with permission from Ref. [24], © Springer Nature Limited 2019. (e) The polynuclear Fe_4 cluster, featuring super exchange to isolate an HS ($S = 5$) ground state. Reproduced with permission from Ref. [28], © Springer Nature Limited 2009. (f) The Fe_4H derivative, a model system demonstrating retained magnetic properties on its surface. Reproduced with permission from Ref. [29], © American Chemical Society 2019.

entropy. The balance between these contributions, modulated by the ligand field and cooperative elastic interactions within the lattice, determines the sharpness, completeness, and hysteresis of the SCO transition. These features collectively render SCO compounds reversible molecular switches, a functionality central to potential applications in sensing, memory, and optoelectronics.

A canonical model is $Fe(phen)_2(NCS)_2$ (phen = 1,10-phenanthroline and NCS = thiocyanate, Fig. 2(a)). At low temperatures, a large t_{2g}-e_g splitting stabilizes the LS configuration, but upon heating, the effective ligand field weakens, and the system converts to the HS state. Accompanying bond-length and bond-angle adjustments dynamically tune the ligand field, enabling reproducible cycling [30]. Complementing the thermal benchmark in Fig. 2(a), Fig. 2(b) highlights the mechanistic pathway of light-triggered SCO in the prototypical FeN_6 chromophore $[Fe(bpy)_3]^{II}$. Photoexcitation initially populates a metal-to-ligand charge-transfer manifold that couples nonadiabatically to the HS potential surface through vibronic interactions. Population of the antibonding e_g orbitals shifts the Fe–N equilibrium to longer distances, creating a structural driving force that traps the system in the HS state. The subsequent motion along the breathing coordinates rapidly dephases, suppressing back transfer to the charge-transfer manifold and dissipating excess energy into the environment. Thus, the electronic population transfer and nuclear rearrangement are temporally distinct yet strongly coupled, leading to one-way structural capture on the HS surface. This sequence provides a microscopic basis for the spin-lattice interplay and clarifies how local coordination geometry changes propagate into cooperative responses to thermal excitation [31]. Extending this framework, Fig. 2(c) highlights SCO in supramolecular Fe^{II}-2,6-bis(1H-pyrazol-1-yl)pyridine (Fe^{II}-BPP) chromophores designed for single-molecule junctions. The underlying mechanism hinges on a balance between ligand field strength and pairing energy: The tensile deformation along the coordination axis increases the Fe–N distances, lowers the ligand field splitting energy (Δ_{CF}) approximately as an inverse power of bond length, and drives the transition from an LS configuration with filled t_{2g} orbitals to an HS configuration with populated antibonding e_g orbitals. In isolated junctions, this deformation-controlled shift in orbital energies switches both the spin state and transport character, with the LS manifold supporting higher off-resonant transmission near the Fermi level, whereas the HS manifold yields spin-selective channels activated at larger energetic offsets. In condensed phases, the same electronic rearrangement couples to weak yet collective elastic interactions, so that subtle changes in intermolecular packing can transform a gradual transition into step-like or abrupt profiles. Interfaces further tune the balance by modifying the ligand field strength and the effective stiffness of the coordination cage, which explains why the junction geometry, anchoring chemistry, and interfacial polarizability critically govern both the efficiency and the reversibility of mechanically assisted crossover. These insights motivate device design strategies that emphasize axial compliance in the metal-ligand scaffold, anchoring groups enforcing longitudinal alignment across the gap, and supramolecular motifs that suppress uncontrolled polymorphism while preserving cooperative amplification of the local spin changes [32].

Recent efforts have further expanded to multinuclear architectures (Fig. 2(d)), where the metal–metal communication mediated by bridging ligands introduces additional degrees of freedom and can markedly reshape the cooperative SCO response. Representative systems such as $[Fe^{II}(Mebik)_2(NCS)_2]$ (Mebik = bis(1-methylimidazol-2-yl)ketone) illustrate how concerted intersite interactions enhance the switchability, extend the apparent blocking of a specific spin state over a broader temperature window, and improve the fatigue resistance under repeated cycling. Through judicious integration of the ligand design (donor type, rigidity, and symmetry), counterion and solvation control, and the selection between mono- and polymetallic motifs, SCO compounds can be engineered to deliver robust, reversible, and stimulus-selective switching, thereby advancing their prospects as functional elements

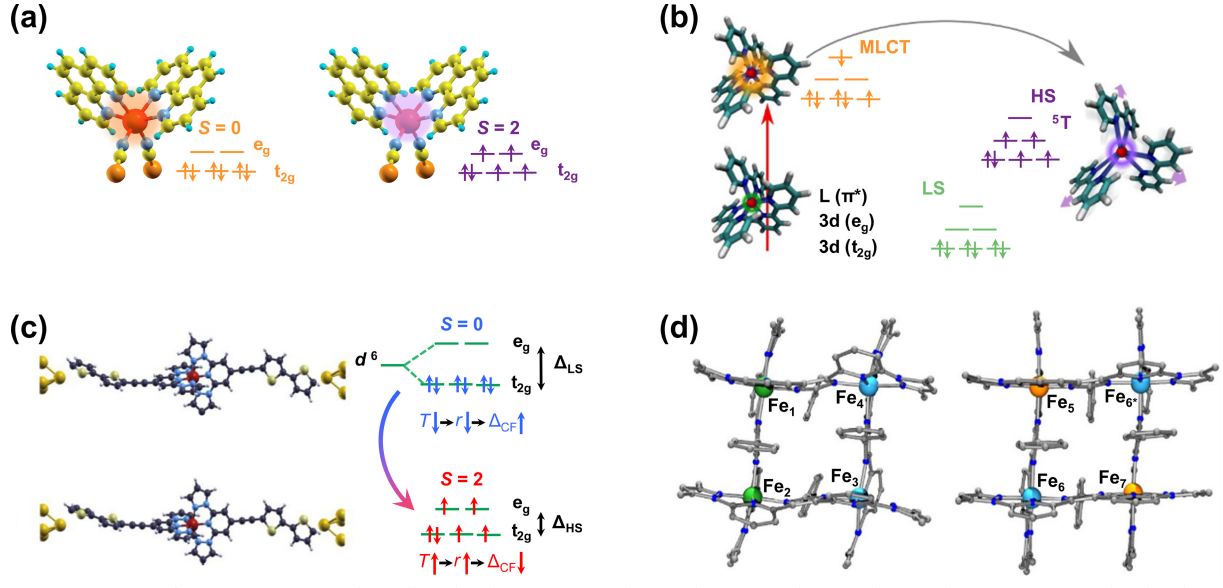

Figure 2 Design strategies for SCO systems. (a) Thermally induced spin state switching in the mononuclear complex $Fe^{II}(phen)_2(NCS)_2$. Reproduced with permission from Ref. [30], © Miyamachi, T. 2012. (b) Light-induced excitation to the HS state in the cationic complex $[Fe(bpy)_3]^{II}$. Reproduced with permission from Ref. [31], © Lemke, H. T. et al. 2017. (c) Mechanical modulation of the spin state in a supramolecular Fe^{II}-BPP junction under stretching. Reproduced with permission from Ref. [32], © Kuppusamy, S. K. et al. 2022. (d) Enhanced cooperativity via ligand engineering and metal-metal communication in the multinuclear SCO framework $[Fe^{II}(Mebik)_2(NCS)_2]$. Reproduced with permission from Ref. [33], © Macmillan Publishers Limited 2014.

in molecular switches, data-storage components, and broader molecular-electronic platforms [33].

2.3 Chiral molecules

Chiral molecules exhibit pronounced selectivity during electron transport, a feature of direct relevance to spintronics and quantum information technologies. This behavior is attributed to the chiral-induced selectivity effect, which enables selective filtering by the molecular chiral structure. At the microscopic level, CISS originates from the breaking of spatial inversion symmetry inherent in molecular chirality, combined with the influence of spin-orbit interactions. The application of an external bias further breaks the time-reversal symmetry, thereby correlating the preferred transport direction with the molecular handedness. Under such conditions, transport through a given enantiomer becomes selectively polarized, with the magnitude and sign of this polarization determined by the molecular structure and the external driving parameters. In this context, chiral systems offer a route to modulate transport without conventional magnetic components, underscoring their potential for spintronic and quantum-information applications.

Figure 3 summarizes representative classes of molecular chirality that underpin CISS-driven transport. Figure 3(a) illustrates point-chiral molecules, typically centered on a chiral carbon atom bonded to four different substituents, forming non-superimposable enantiomers. These motifs are ubiquitous in natural compounds (such as amino acids and sugars) and play vital roles in biomolecular recognition and materials science [34]. Electron transmission through these molecules exhibits significant selectivity that can be tuned by external stimuli like light or electric fields. Axially chiral molecules, shown in Fig. 3(b), arise from restricted rotation around a chiral axis, resulting in stable enantiomers [35]. This geometry, commonly observed in helicenes and certain coordination complexes, enables directional transport, highlighting their potential for spintronic applications. Figure 3(c) presents planar-chiral ferrocene derivatives, in which chirality originates from the specific spatial arrangement of the central metal atom and its cyclopentadienyl ligands [36]. These compounds frequently show the excellent filtering performance and serve as platforms for molecular switches and catalytic studies. In Fig. 3(d), DNA is highlighted as a prototypical helical-chiral system. Its inherent double-helix architecture, prevalent in biological systems, endows it with intrinsic handedness and strong selectivity, enabling the helical framework to significantly influence the electron spin behavior during charge transport [37]. Figure 3(e) finally shows overcrowded alkenes, which can undergo reversible right- (P)/left-handed (M) helicity inversion driven by light or heat. By switching molecular handedness and coupling this conformational change to spin-orbit

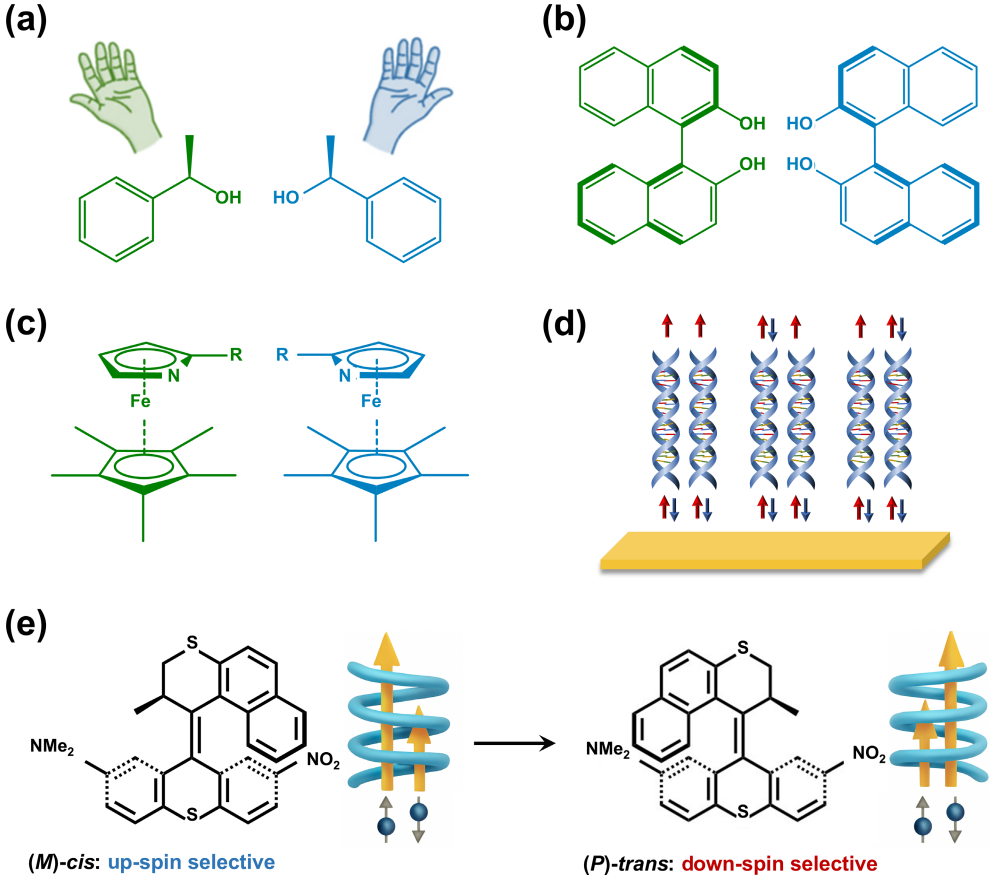

Figure 3 Classes of molecular chirality. (a) Central chirality, exemplified by amino acids with stereogenic centers. Reproduced with permission from Ref. [34], © Bousquet, E. et al. 2025. (b) Axial chirality, as in helicenes, with rotational asymmetry enabling direction-dependent filtering. Reproduced with permission from Ref. [35], © Pu, L. 2024. (c) Planar chirality, illustrated by ferrocene derivatives, showing high polarization from asymmetric ligand-metal geometry. Reproduced with permission from Ref. [36], © IUPAC 2001. (d) Helical chirality, represented by DNA, with its double-helix architecture enabling intrinsic electron transport with selectively. Reproduced with permission from Ref. [37], © The American Association for the Advancement of Science 2011. (e) Switchable chiral systems, such as overcrowded alkenes, with reversible helicity inversion under optical or thermal stimuli enabling tunable filtering direction. Reproduced with permission from Ref. [38], © Suda, M. et al. 2019.

interactions, these molecules can reverse the direction of polarization. This optically and thermally addressable filtering behavior provides a route to reconfigurable spin filters and expands the design possibilities for chirality-based spin control in molecular spintronics [38].

2.4 Organic radical molecules

Organic radical molecules, owing to their unique magnetic properties, have emerged as focal systems for molecular electronics and spintronics. These radicals possess at least one unpaired electron in their ground state, endowing them with a magnetic moment that governs both magnetic response and charge-transport behavior under external electric or magnetic fields. Depending on charge state, molecular architecture, and environment, radicals can exhibit paramagnetic, antiferromagnetic, or ferromagnetic responses, offering a versatile platform for conduction, gating, and readout at the single-molecule level. Transport in these systems typically proceeds by off-resonant tunneling or thermally assisted hopping and is highly sensitive to the alignment of the singly occupied molecular orbital (SOMO) with electrode Fermi levels and interfacial hybridization. A canonical benchmark is the triphenylmethyl (trityl) radical (Fig. 4(a)), in which three phenyl rings provide steric protection that stabilizes carbon center, while the aryl framework delocalizes the unpaired electron sufficiently to suppress bimolecular recombination yet retain a well-defined magnetic moment [39]. These features enable chemically robust and spin-polarized transport suitable for conductance control and quantum-spin studies, including ESR-addressable junctions. In contrast, viologen radical cations (Fig. 4(b)) are generated electrochemically via redox conversion and exhibit pronounced electronic effects during charge transfer. Their distinct optical signatures across redox states support applications in electrochromic devices, while the interfacial exchange with electrodes offers opportunities to tune electronic injections and rectification [40]. The tetracyanoquinodimethane (TCNQ) radical anion (Fig. 4(c)) represents another archetype whose strong π-acceptor character yields characteristic conductance fingerprints. Its stability and electronic transport have motivated widespread use in molecular materials, charge-transfer assemblies, and device heterojunctions requiring strong magnetic responses [41].

Further notable systems underscore how interfacial physics and molecular design co-determine electron transport. Polychlorotriphenylmethyl (PTM) radicals (Fig. 4(d)) function as molecular sensors in solid-state junctions: Quantum-transport measurements reveal a stable zero-bias Kondo resonance when the localized magnetic moment couples antiferromagnetically to conduction electrons in metallic electrodes, with the resonance amplitude and width tracking the Kondo temperature (T_K) and its splitting under a magnetic field [42]. {4-[{[2,5-Bis(4-sulfanylphenyl[eth-1-yn-2-yl])phenyl]carbonyl}(methyl)amino]-2,2,6,6-tetramethyl piperidin-1-yl}oxidanyl (TEMPO-OPE) (Fig. 4(e)) constructs highlight radical-induced modulation of conductance through positive magnetoresistance (MR). Field-dependent alignment of the TEMPO spin and associated changes in scattering at the metal-molecule contact invert the more common negative response, underscoring the role of interfacial exchange and anchor chemistry in setting the magnetotransport sign and magnitude [43]. Finally, phenothiazine (PTZ) radicals (Fig. 4(f)), produced via redox activation, combine the high chemical stability with enhanced conductance. Narrowing of the highest occupied molecular orbital–lowest unoccupied molecular orbital (HOMO–LUMO) gap lowers the tunneling barrier and shifts transport toward the near-resonant regime, yielding larger currents at modest bias. Collectively, these examples show that tailored electronic structures (such as SOMO energy, conjugation length, and donor–acceptor asymmetry) together with magnetic moments provide powerful means to engineer spin-selective transport. Practical design principles include: (1) controlling redox state and counterions to place the SOMO near the electrode Fermi level; (2) selecting rigid and π-conjugated backbones to reduce spin-phonon decoherence while maintaining sufficient delocalization for stability; (3) engineering electrode coupling through thiol, amine, or carbene anchors, and using Au, graphene, or ferromagnetic contacts to tune exchange and spin injection; and (4) exploiting molecular symmetry to suppress destructive spin interference. With these strategies, organic radicals enable reconfigurable spin

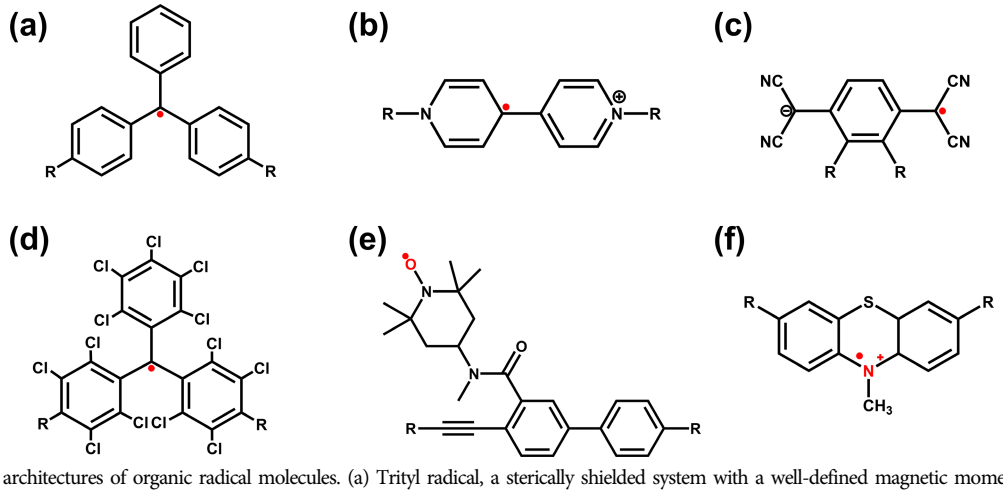

Figure 4 Molecular architectures of organic radical molecules. (a) Trityl radical, a sterically shielded system with a well-defined magnetic moment. Reproduced with permission from Ref. [39], © American Chemical Society 2023. (b) Viologen radical cation, a redox-active unit for tunable electronic injection. Reproduced with permission from Ref. [40], © Wiley-VCH Verlag GmbH & Co. KGaA, Weinheim 2017. (c) TCNQ radical anion, a strong π-acceptor for charge-transfer complexes. Reproduced with permission from Ref. [41], © Elsevier 2019. (d) PTM radical, exhibiting a robust Kondo resonance as a molecular sensor. Reproduced with permission from Ref. [42], © American Chemical Society 2015. (e) TEMPO-OPE radical, a molecular wire displaying positive magnetoresistance. Reproduced with permission from Ref. [43], © American Chemical Society 2016. (f) PTZ radical, a high-conductance system with a narrow HOMO–LUMO gap. Reproduced with permission from Ref. [44], © Wiley-VCH Verlag GmbH & Co. KGaA, Weinheim 2017.

filters, molecular switches, and hybrid quantum-optoelectronic platforms, while advancing fundamental understanding of spin coherence, interfacial exchange, and many-body effects at the molecular scale [44].

Taken together, the four molecular archetypes discussed above address complementary aspects of spin functionality at the single-molecule level, ranging from long-lived spin memory and stimulus-responsive bistability to efficient spin polarization and spin-dependent charge transport. Although each platform excels within a specific operational regime, their practical implementation depends on a balanced interplay of stability, tunability, accessible temperature range, and device compatibility. To facilitate a direct comparison of these key characteristics, a concise summary is provided in Table 1 below.

3 Single-molecule spin-related effects

The structural diversity of single-molecule spin systems, including SMMs, SCO complexes, chiral molecules, and organic radicals, gives rise to distinct spin characteristics determined by their unique orbital configurations and electron distributions. These systems not only offer atomically programmable architectures but also serve as ideal platforms for probing quantum spin phenomena. As an intrinsic degree of freedom, electron spin is emerging as a central design variable for molecular-scale functional devices, offering control modalities that far exceed those available in charge-based mechanisms. This chapter focuses on spin-related effects in single-molecule systems, including representative mechanisms such as the Kondo effect, Zeeman splitting, spin coupling, SCO, spin filtering, spin caloritronics, and interface-induced spin behavior. We aim to elucidate how these quantum mechanisms govern electron transport at the microscopic level and thereby enable the realization of tailored device functionalities.

To help navigate this broad landscape, it is useful to distinguish these spin-related effects by their underlying physical origins and corresponding experimental signatures. The single-molecule Kondo effect is a many-body screening phenomenon, characterized by a zero-bias conductance peak that sharpens and intensifies upon cooling and splits under an applied magnetic field. Spin coupling arises from exchange interactions between localized molecular spins, and is usually manifested as bias- or gate-dependent inelastic spin-flip excitations or singlet-triplet level crossings. SCO involves a ligand-field-driven bistable transition between HS and LS configurations, which can lead to discrete conductance switching and, in some cases, hysteresis as a function of temperature, electric field, or mechanical strain. Spin filtering denotes spin-selective electron transmission through a single molecule, quantified by spin polarization or MR. This effect can originate from mechanisms such as magnetic orbital splitting, spin-state reconfiguration, quantum interference, or CISS; the latter represents a unique non-magnetic case where chiral molecules generate spin-polarized currents without an external magnetic field. Spin caloritronic effects, driven by thermal gradients, are identified by finite spin currents or spin-dependent Seebeck coefficients under conditions of near-zero net charge current. Finally, interface-induced spin behavior arises from the symmetry, chemistry, and coupling strength at the molecule-electrode contacts, often leading to geometry-sensitive MR, anisotropic spin responses, or competition between Kondo screening and spin polarization. In the subsequent subsections, we will discuss each effect in detail, emphasizing how their distinct microscopic origins translate into experimentally resolvable transport signatures.

3.1 Single-molecule Kondo effect and Zeeman effect

In condensed matter physics, the Kondo effect refers to the characteristic low-temperature resistance minimum observed in metals containing magnetic impurities [8]. This phenomenon arises from many-body quantum screening, whereby conduction electrons collectively screen a localized magnetic moment. The Anderson impurity model provides a standard theoretical description of such a system (Fig. 5(a)) [45]. The impurity is modeled as a localized orbital with a single electron at energy ε_0. When ε_0 lies below the Fermi level, the unpaired electron constitutes a localized spin-1/2 magnetic moment. Although classically fixed, quantum fluctuations allow virtual processes in which an electron tunnels from the impurity to the electrode, while being replaced by another electron from the Fermi sea with arbitrary spin. The coherent superposition of such events leads to the formation of a Kondo singlet and a resonance at the Fermi level.

At the single-molecule level, the Kondo effect manifests as a zero-bias conductance peak, known as the Kondo resonance. When molecules with non-zero spin such as radicals or SMMs are bridged between metallic electrodes, their local moments couple antiferromagnetically to the conduction electrons, inducing a many-body correlated state [8]. This dynamic screening process forms a "Kondo cloud" of electrons with opposite spin near the Fermi level (Fig. 5(b)), effectively quenching the molecular magnetic moment. The process is enabled by Coulomb blockade and the Pauli

Table 1 Stability, tunability, operating temperature, and device compatibility of representative single-molecule spin systems

Molecular system	Stability	Tunability	Operating temperature	Device compatibility
SMMs	High magnetic anisotropy for stable spin states; high feasibility of surface preservation	Ligand-field and crystal-field engineering; metal-ion selection; exchange-coupling architecture design	Predominantly cryogenic; blocking temperature below room temperature	Demonstrated surface/junction integration; limited room-temperature scalability.
SCOs	Well-defined LS/HS bistability; cooperative stabilization via intermolecular interactions	Stimuli-responsive control (e.g., thermal, optical, mechanical, and electrochemical)	Room temperature for thermal SCO; low temperature required by photo-induced states	Strong potential for switches and memory; reproducibility limited by interface and dynamics
CISS	Inherently stable molecular chirality; persistent spin selectivity under ambient conditions	Chirality, length, and anchoring group variation; dependence on bias and electrode magnetization	Broad range, including room temperature; no magnetic ordering required	Broad junction/device compatibility; quantification limited by interfacial control
Organic radicals	Stable open-shell ground states; robust spin/charge transport signatures	Magnetic field, redox state, and electrostatic gating (platform-dependent)	Cryogenic (many-body effects) to room temperature (redox conduction)	Compatibility with MCBJ/EMBJ platforms; variability due to interfacial sensitivity

exclusion principle, allowing spin-flip tunneling without net charge transfer.

The energy scale of this many-body screening is defined by T_K, given by [46]

$$T_K = 0.5(\Gamma E_C)^{1/2}\exp(-\pi\varepsilon/\Gamma) \quad (1)$$

where Γ denotes the hybridization strength between molecular orbitals and electrodes, E_C is the effective charging energy, and ε is the energy offset of the orbital from the Fermi level. Strong Kondo coupling arises when $T \ll T_k$, enhancing the density of states (DOS) near E_F and producing a pronounced zero-bias peak in differential conductance spectra (Fig. 5(c)) [42]. As temperature decreases, this resonance increases in height and narrows in width, serving as a key experimental signature.

In HS or multi-channel systems, richer Kondo physics emerges [47]. For instance, MnPc molecules exhibit two-stage Kondo screening due to intramolecular spin dimers formed by orbitals such as d_{z^2} and $d_{x^2-y^2}$ [48]. This leads to a temperature-dependent evolution from a broad single peak above 3 K, through an intermediate phase with suppressed conductance between 0.3 and 3 K, to split peaks below 0.3 K, reflecting interference between spin channels and the formation of a secondary Kondo singlet (Fig. 5(d)). The secondary Kondo temperature (T^*) depends linearly on the intramolecular spin-exchange strength, indicating molecular-level control over correlated quantum phases.

The response to external magnetic fields provides direct access to spin degeneracy and quantum coherence [46, 49]. Via the Zeeman effect, magnetic fields lift spin degeneracy by splitting energy levels according to

$$\Delta E = g_{\text{eff}}\mu_B B m_s \quad (2)$$

where g_{eff} is the effective Landé factor, μ_B is the Bohr magneton, and m_s is the spin projection quantum number. In single-molecule systems, g-factor anisotropy and spin-orbit coupling (SOC) lead to direction-dependent Zeeman splitting and nontrivial g_{eff} values. When $g_{\text{eff}}\mu_B B > k_B T_k$, the zero-bias peak splits into two or more sub-peaks with spacing

$$\Delta V = g_{\text{eff}}\mu_B B/e \quad (3)$$

Systems with S = 1/2 show symmetric double peaks, whereas systems with S = 1 exhibit triplet structures under axial magnetic fields (Fig. 5(e)) [50]. The splitting behavior and peak heights serve as precise indicators of spin states and magnetic-field strength, enabling reversible and gate-tunable manipulation of molecular spin via electrode hybridization and orbital control.

As mentioned above, the single-molecule Kondo effect reveals profound many-body quantum correlations and enables external control of spin states via electric and magnetic fields. The ability to tune Kondo resonances through parameters such as temperature, magnetic field, gate voltage, and molecule-electrode coupling highlights its potential for realizing addressable molecular spin qubits and programmable spintronic devices, with direct implications for molecular-scale quantum technologies [51–58].

3.2 Single-molecule spin coupling effect

Single-molecule spin coupling refers to coherent interactions among multiple localized spin centers within a molecule, typically mediated by magnetic exchange or electron delocalization [59]. At

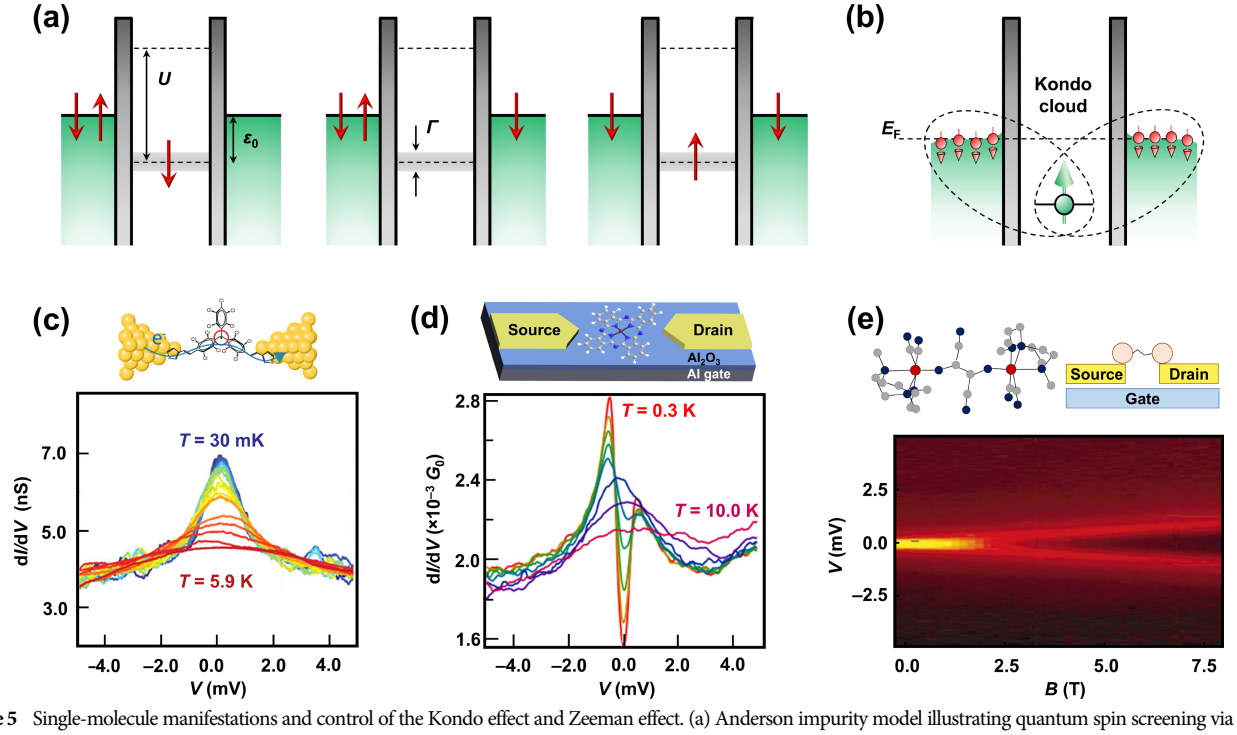

Figure 5 Single-molecule manifestations and control of the Kondo effect and Zeeman effect. (a) Anderson impurity model illustrating quantum spin screening via virtual tunneling, forming a Kondo singlet near the Fermi level. Reproduced with permission from Ref. [45], © American Chemical Society 2010. (b) Kondo cloud in a single-molecule junction, showing conduction-electron screening of a localized spin. Reproduced with permission from Ref. [8], © Springer Nature Limited 2019. (c) Temperature-dependent Kondo resonance, observed as a sharpening zero-bias conductance peak. Reproduced with permission from Ref. [42], © American Chemical Society 2015. (d) Two-stage Kondo screening in MnPc, showing peak splitting with decreasing temperature. Reproduced with permission from Ref. [48], © Guo, X. et al. 2021. (e) Magnetic-field-induced Zeeman splitting of the Kondo peak, reflecting spin states and g-factor anisotropy. Reproduced with permission from Ref. [50], © Macmillan Magazines Ltd. 2002.

the microscopic level, this coupling arises from exchange interactions between localized orbitals and is commonly described by a Heisenberg-type spin Hamiltonian, $H = -J\vec{s_1} \cdot \vec{s_2}$, where the sign and magnitude of the exchange parameter J determine whether the coupling is ferromagnetic or antiferromagnetic [60]. Spin centers may originate from transition-metal ions, organic radicals, or unpaired electrons in π-conjugated systems. Coupling mechanisms include direct exchange, superexchange, or indirect interactions such as Ruderman–Kittel–Kasuya–Yosida (RKKY) coupling mediated by conduction electrons [61, 62]. These interactions not only reveal intrinsic molecular magnetism but also form the basis for molecular-scale spintronic devices, qubits, and magnetic switches. Experimental and theoretical studies have demonstrated that such couplings are highly sensitive to molecular structure, radical positioning, charge state, electrode coupling geometry, and external electric fields.

A clear example of electrically tunable spin coupling was demonstrated in a dicobalt single-molecule junction, where two Co^{II} ions (HS d^7) are bridged by a ligand [59]. As shown in Fig. 6(a), the two spins form near-degenerate pseudo singlet and pseudo triplet states separated by an energy gap of 2–3 cm^{-1} (Fig. 6(b)), which is highly sensitive to the applied bias. At low bias, this leads to interfacial charge redistribution, reconstructing the exchange pathway and stabilizing the triplet state, which then dominates electron transport and induces a Kondo resonance and a zero-bias anomaly (Fig. 6(c)). This behavior reflects the electric-field tunability of intramolecular magnetic states.

To explain this phenomenon, a nonequilibrium transport model was developed [60]. As illustrated in Fig. 6(d), the system comprises two molecular orbitals, with one fixed at ε_0 and the other coupled via a tunneling interaction τ_c, forming hybridized levels at $\varepsilon_0 \pm \tau_c$. The effective exchange coupling J scales with the molecule–electrode hybridization strength Γ. At zero bias, if the Fermi level lies between the hybridized states, the system favors a delocalized triplet (ferromagnetic) configuration. Applying a bias shifts the chemical potentials, altering orbital occupancy and reversing the sign of J, thus favoring an antiferromagnetic and localized regime. This transition suppresses conductance due to spin blockade. Importantly, this model reveals that exchange coupling is not only determined by molecular structure but can also be dynamically tuned by external electric fields, enabling electric-field-driven spin-state switching without magnetic assistance.

In metal-free systems, all-organic diradical junctions have emerged as versatile platforms for studying spin interactions [61]. In the system shown in Fig. 6(e), two radicals are connected via a rigid π-conjugated backbone. At low temperatures, IETS reveals spin-flip excitations in the coupled state, whereas decoupled states or geometric distortions result in Kondo resonances. These observations confirm that the coupling strength depends critically on orbital symmetry, radical separation, and the structure of the π-conjugated framework, opening pathways toward mechanical control of spin order.

More sophisticated control has been achieved in redox-active organic diradicals, where a gate voltage modulates both the charge state and spin configuration [63]. As shown in Fig. 6(f), two methyl radicals linked by a benzene ring form an antiferromagnetic state (J_{12} = 4.65 meV) in the neutral charge state (charge state = 0), evidenced by symmetric IETS steps at ± 4.65 mV. Applying a gate voltage injects an electron into an unoccupied orbital on the ring, forming a tri-spin system (charge state = −1) with unequal superexchange couplings (J_{13} = 2 meV and J_{23} = 23 meV). This reconfiguration leads to new IETS excitations and a zero-bias Kondo peak. This charge-induced spin reconfiguration occurs on picosecond timescales, suggesting potential applications in

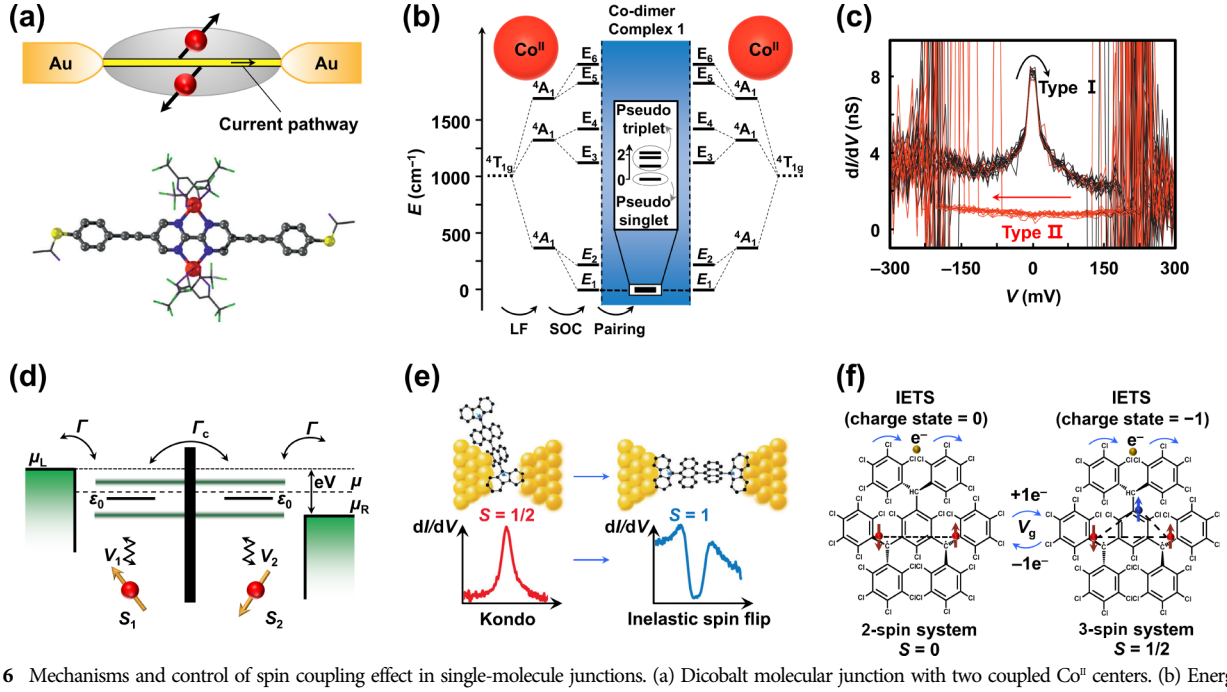

Figure 6 Mechanisms and control of spin coupling effect in single-molecule junctions. (a) Dicobalt molecular junction with two coupled Co^{II} centers. (b) Energy-level diagram showing a near-degenerate pseudo singlet and pseudo triplet with bias-dependent splitting. (c) Bias-induced singlet-triplet transition leading to Kondo resonance and zero-bias anomaly. Reproduced with permission from Ref. [59], © Springer Nature Limited 2013. (d) Nonequilibrium transport model demonstrating bias-tunable exchange coupling. Reproduced with permission from Ref. [60], © American Chemical Society 2016. (e) All-organic diradical junction exhibiting geometry-dependent spin-flip excitations and Kondo features. Reproduced with permission from Ref. [61], © Baum, T. Y. et al. 2022. (f) Redox-controlled diradical enabling gate-switchable spin-configuration transitions for reprogrammable molecular spin logic. Reproduced with permission from Ref. [63], © American Chemical Society 2017.

quantum SWAP gates (the fundamental two-qubit gates that exchange quantum states) and programmable molecular spin logic.

Overall, single-molecule spin coupling integrates orbital-level exchange, nonequilibrium spin dynamics, and field-tunable correlations. Spanning diverse systems from metal complexes to purely organic radicals, it offers promising functionality for molecular-scale quantum devices, spin-logic architectures, and reconfigurable memory elements.

3.3 Single-molecule spin crossover effect

In single-molecule spintronic devices, the SCO effect reveals a unique quantum dynamical behavior that extends beyond its classical thermodynamic nature in bulk materials [30]. At the molecular scale, the SCO effect arises from the competition between Δ_{CF} and electron pairing energy (E_P), which collectively determine d-orbital electron configurations [64]. As illustrated in Fig. 7(a), weak ligand fields ($\Delta_{CF} < E_P$) favor HS states due to dominant electron-electron repulsion, while strong fields ($\Delta_{CF} > E_P$) stabilize LS states by overcoming E_P. Near the crossover region where $\Delta_{CF} \approx E_P$, HS and LS states become nearly degenerate, enabling spin transitions via subtle perturbations.

In single-molecule devices, the SCO behavior cannot be fully described by traditional ligand field theory. Instead, it involves multi-scale mechanisms such as molecule-environment coupling, electron–phonon interactions, and quantum tunneling. Although the electronic structure dominates the transport behavior, the molecule–electrode interface may obscure intrinsic spin properties [30]. To address this complexity, an Ising-like model has been developed to extend thermodynamic descriptions by incorporating cooperative coupling, successfully explaining hysteresis and field-driven spin transitions [65]. The model Hamiltonian is given by

$$H = -J\sum_{i,j} S_i S_j + \sum_i \left(\frac{\Delta_i}{2} - k_B T \ln g_i \right) S_i \quad (4)$$

Here, S_i is a discrete spin state (LS: −1, and HS: +1), Δ_i is the local energy gap, and g_i accounts for the spin degeneracy ($g_{HS} > g_{LS}$). This model captures the hysteresis behavior observed when heating and cooling follow different spin-transition pathways [66]. This bistability renders SCO molecules promising for data storage, where their spin states can remain stable against environmental fluctuations.

Achieving precise spin state control at the molecular level is essential for future molecular spin devices [65]. Among various external stimuli, the mechanical force is particularly effective due to its direct action on molecular geometry. By modifying the coordination environment, mechanical deformation tunes the ligand field and thus the spin state. In Fig. 7(b), an Fe-porphyrin molecule is positioned between an STM tip and a substrate. Adjusting tip height applies atomic-scale tensile or compressive strain [67]. As the molecular junction is stretched, the macrocyclic ligand flattens, Fe–N bonds contract, and a spin transition from S = 2 to S = 1 occurs. The Kondo resonance width increases significantly and reverses repeatedly (Fig. 7(c)), indicating reversible magnetic switching. First-principles calculations confirm that this transition is driven by ligand field enhancement rather than charge transfer. Control experiments confirmed that tunneling-induced displacements without full mechanical coupling are insufficient to trigger the spin transition, highlighting the essential role of mechanically induced conformational change.

In comparison with temperature, light, or mechanical force, electric fields offer faster response speeds, strong spatial localization, and superior device integrability, making them ideal for SCO manipulation. Electric fields influence the SCO effect through

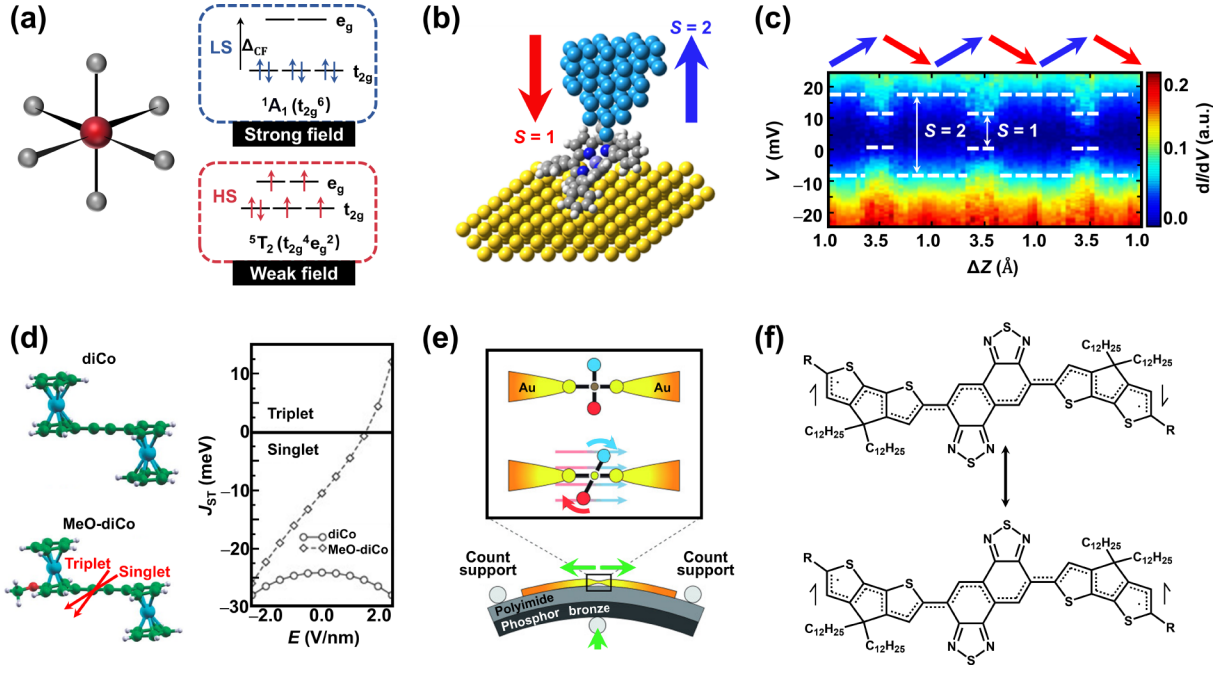

Figure 7 Mechanisms and control of the SCO effect in single-molecule junctions. (a) Ligand field theory diagram of the HS/LS crossover. Reproduced with permission from Ref. [64], © WILEY-VCH Verlag GmbH & Co. KGaA, Weinheim 2017. (b) STM-based mechanical control of an Fe-porphyrin junction via tip-induced stretching. (c) Reversible spin switching from S = 2 to S = 1, indicated by Kondo resonance modulation. Reproduced with permission from Ref. [67], © American Chemical Society 2017. (d) Density functional theory-predicted electric-field control of spin switching in a diiron π-bridged complex via orbital reordering. Reproduced with permission from Ref. [69], © Springer Nature Limited 2009. (e) Electric-field-induced geometric distortion in Fe^{II}-terpyridine with push–pull dipoles. Reproduced with permission from Ref. [71], © Wiley-VCH Verlag GmbH & Co. KGaA, Weinheim 2015. (f) Singlet-triplet transitions in NTCPhN with open-shell configurations. Reproduced with permission from Ref. [72], © Yang, C. Y. et al. 2024.

several mechanisms: directly modifying Δ_{CF}, inducing conformational distortions via dipolar interactions, and shifting orbital occupancy and charge localization [68].

Early theoretical studies predicted that electric fields could regulate the relative stability of spin states in molecules by introducing a dipole effect, thereby inducing the SCO effect. As shown in the left panel of Fig. 7(d), symmetric dicobaltocene (diCo) molecules, due to the lack of a permanent dipole moment, do not exhibit crossing between the singlet and triplet states under an applied electric field, showing stable antiferromagnetic coupling [69]. However, when a polar substituent (e.g., MeO) is introduced on one side, the resulting MeO-diCo molecule displays a noticeable dipole, breaking the inversion symmetry and producing a first-order Stark effect in response to the electric field. The right panel of Fig. 7(d) shows the variation of the exchange coupling constant J_{ST} with electric field strength: In diCo, J_{ST} remains negative, corresponding to an antiferromagnetic state. In contrast, in MeO-diCo, when the electric field strength reaches a critical value of approximately 1.5 V/nm, the singlet and triplet states become degenerate, leading to the SCO effect from the antiferromagnetic to the ferromagnetic state. During this process, the electric field acts on the molecular dipole, altering the energy levels of the local orbitals, which changes the sign of the exchange coupling between the magnetic centers. This effect has been similarly verified in other dicobaltocene derivatives with asymmetric polar substituents.

Subsequent studies expanded the electric field regulation mechanism by exploring direct modulation of the spin state at the transition metal center via gate voltage. For example, adjusting the gate voltage to control the electronic state of the terpyridine ligand allows effective control of the ligand field strength around the transition metal ion (such as Mn^{II}), achieving a transition from HS ($S = 5/2$) to LS ($S = 1/2$) [70].

Further investigations revealed that the electric field regulates the SCO effect by inducing geometric distortions in the coordination sphere. As shown in Fig. 7(e), in an Fe^{II}-terpyridine single-molecule junction fabricated using MCBJ, the ligand structure deforms under the electric field, changing the coordination environment of the metal ion [71]. This weakens the ligand field strength, reducing Δ_{CF} and triggering a transition from LS ($S = 0$) to HS ($S = 2$). When the electric field reaches a certain threshold, the spin state changes significantly, and the current response exhibits clear bistable behavior.

Beyond the conventional metal-centered spin-crossover systems described above, recent research has revealed an expanded manifestation of SCO in purely organic open-shell molecules, where the spin transition arises not from variations in metal-ligand orbital splitting but from intrinsic electronic correlations within π-conjugated frameworks [72]. In a graphene–molecule–graphene single-molecule junction, an open-shell donor–acceptor diradical based on a naphtho[1,2-c:5,6-c]bis([1,2,5]thiadiazole) (NTCPhN) derivative was covalently bonded to graphene electrodes through amide linkages, creating a stable and well-controlled interface that preserves the intrinsic spin activity of the molecule. Time-resolved transport measurements identified three discrete conductance states, corresponding to the closed-shell singlet, open-shell singlet, and open-shell triplet configurations (Fig. 7(f)). The relative populations of these states can be tuned simultaneously and cooperatively by temperature, electric field, and magnetic field. Thermal excitation enhances the population of the triplet state, the applied bias alters the energy alignment and activation barriers, and an external magnetic field promotes singlet-triplet conversion accompanied by pronounced magnetoresistance at low temperatures. Unlike the orbital-driven SCO observed in transition-metal complexes, this phenomenon showcases multi-stimuli and device-integrated control of spin multiplicity in a metal-free diradical system, extending the concept of spin crossover from its classical definition to a broader regime governed by electronic correlation.

Generally speaking, the SCO effect has evolved from a bulk thermodynamic phenomenon into a molecular-scale quantum effect. The ability to cooperatively control spin state, orbital structure, and molecular geometry via mechanical or electric stimuli reveals new dimensions of SCO physics and provides a solid foundation for designing programmable, low-power, and integrated single-molecule spintronic devices [73, 74].

3.4 Single-molecule spin filtering effect

Single-molecule spin filtering refers to the spin-selective transport behavior observed when electrons tunnel through an individual molecule, exhibiting significantly different transmission probabilities for spin-up and spin-down electrons [75]. This phenomenon embodies a quantum mechanism for spin discrimination at the molecular scale and is quantitatively characterized by the spin polarization ratio (SP) [76]

$$\mathrm{SP} = \frac{|I_{\uparrow} - I_{\downarrow}|}{I_{\uparrow} + I_{\downarrow}} \times 100\% \tag{5}$$

As a central theme in molecular spintronics, spin filtering aims to uncover the origin of spin polarization at the atomic scale and develop methods for its active control in device applications. One direct mechanism for single-molecule spin filtering arises from intrinsic spin splitting in magnetic molecular orbitals [73, 77]. For instance, in Mn–Cu-based SMMs (Fig. 8(a)), spin-dependent orbital energies are modulated by magnetic anisotropy and external bias, creating distinct conduction channels for spin-up and spin-down electrons [78]. At zero bias, the system supports a highly spin-polarized conduction channel. Upon applying a bias voltage, changes in orbital occupancy reverse the spin direction, effectively realizing a voltage-controlled spin switch (Fig. 8(b)).

Another mechanism involves spin state transitions in SCO molecules. In Fe-based SCO systems, the reversible transition between HS and LS states reshapes the molecular orbital energy landscape. In the HS state, spin-selective orbitals may align near the Fermi level, enabling polarized transport. In the LS state, the absence of such alignment suppresses spin selectivity [73]. This spin-orbital coupling can be tuned by temperature, electric fields, or chemical stimuli, offering a non-magnetic route to spin modulation.

Importantly, spin filtering does not always require magnetic species. The CISS effect demonstrates that chiral molecules, in the presence of spin-orbit coupling, can generate spin-polarized currents without external magnetic fields. For example, the spin-selective conduction has been observed in DNA oligomers between non-magnetic electrodes, highlighting the spontaneity and generality of the CISS effect [79]. The underlying mechanism involves spin-orbit coupling between the electron's motion along a helical path and its spin, leading to momentum-spin locking. This creates asymmetric potential barriers for different spin orientations, enabling spin separation.

Building on this non-magnetic paradigm, single-molecule

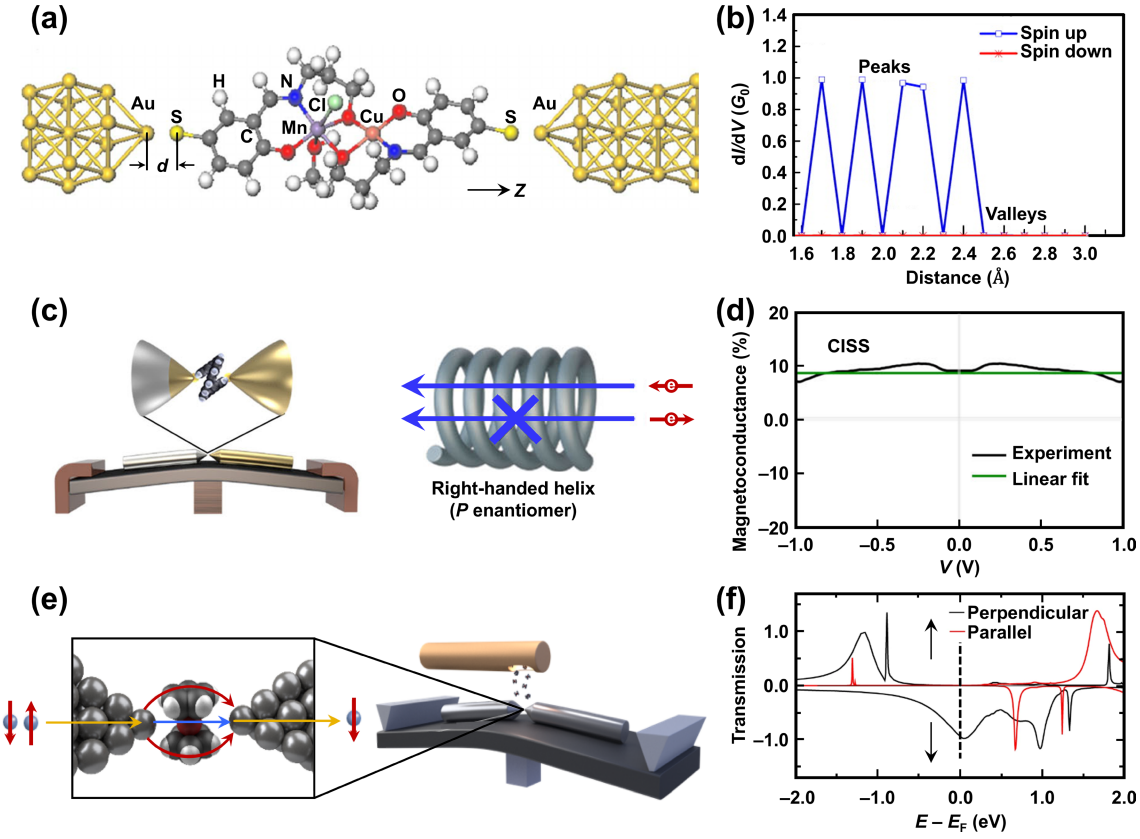

Figure 8 Mechanisms and control of spin filtering effect in single-molecule junctions. (a) Spin filtering in Mn–Cu-based SMMs via spin-split orbitals and magnetic anisotropy. (b) Bias-induced reversal of spin polarization via orbital occupancy changes. Reproduced with permission from Ref. [78], © American Institute of Physics 2010. (c) Helicene-based break-junction device forming a chiral transport channel for measuring CISS. (d) Magnetoconductance reversal with field direction or chirality confirms spin-selective transport. Reproduced with permission from Ref. [80], © Singh, A. K. et al. 2025. (e) Quantum interference-driven spin filtering in an Ag–vanadocene–Ag junction. (f) Spin-resolved transmission spectrum showing nearly perfect spin polarization from quantum interference. Reproduced with permission from Ref. [81], © Pal, A. N. et al. 2019.

junction experiments further demonstrate that CISS-type spin filtering can be directly measured at the atomic scale when a spin-polarized injector is introduced. In helicene-based break-junction devices, an enantiopure 2,2′-dithiol-[6]helicene molecule bridges a ferromagnetic Ni electrode and a non-magnetic Cu, Ag, or Au counter electrode, forming a well-defined chiral tunnelling pathway within an atomic-scale junction geometry (Fig. 8(c)) [80]. The spin-filtering mechanism is consistent with the CISS picture in Fig. 8(c), where the electron transport through a chiral potential favors one spin population and suppresses the opposite one. Experimentally, the magnetoconductance can be decomposed into symmetric and antisymmetric components, and the bias-symmetric component is attributed to CISS, providing a direct signature of spin-selective transmission through a single chiral molecule, as shown in Fig. 8(d).

Beyond magnetic and chiral systems, the quantum interference offers a purely electronic approach to spin filtering. In the Ag–vanadocene–Ag molecular junction (Fig. 8(e)), near-perfect spin polarization was achieved despite the absence of magnetic components or magnetic fields [81]. Calculations revealed two independent electron pathways: one through the vanadium d_{z^2} orbital and the other one through the π-conjugated backbone. These pathways interfere destructively for one spin orientation (spin-up), suppressing transmission, while constructive interference occurs for the opposite spin (spin-down), enabling nearly lossless conduction (Fig. 8(f)). These result in ideal single-channel spin filtering driven solely by orbital symmetry and quantum interference, independent of magnetic order.

In brief, recent advances in single-molecule spin filtering span a range of mechanisms, including magnetic orbital splitting, spin state reconfiguration, CISS, and quantum interference engineering. These mechanisms share a common feature: They exploit the differences in how spin-up and spin-down electrons interact with molecular orbitals, energy alignments, and symmetry-breaking factors at the quantum level. Functionally, such effects enable not only static spin polarization, but also dynamically reconfigurable spin control, paving the way for low-power, high-efficiency, and atomically precise spintronic devices.

3.5 Single-molecule spin thermoelectric effect

The conversion of thermal energy into spin information at the nanoscale has become a significant research direction bridging spintronics and molecular electronics. In the specific context of single-molecule junctions, the spin thermoelectric effect refers to the generation of a spin-polarized current driven by a temperature gradient [82]. A key objective in this area is to achieve a pure spin current, one that carries spin angular momentum without net charge flow. This process relies on the coupling between molecular orbitals and spin states, thermally activated carrier transport, and the construction of spin-selective tunneling pathways.

In the broader context, this phenomenon is categorized into two types: the spin Seebeck effect (SSE), where a temperature gradient

induces a spin current, and the spin Peltier effect (SPE), where a spin current drives the heat flow [83]. Since SPE remains experimentally challenging to realize, current research primarily focuses on SSE, which is often considered synonymous with the spin thermoelectric effect in molecular systems. A central parameter is the spin-dependent Seebeck coefficient S_s, defined as [84]

$$S_s = -\left.\frac{\Delta V_s}{\Delta T}\right|_{I_{ch}=0} \quad (6)$$

where the condition $I_{ch} = 0$ ensures zero charge current. The sign of S_s indicates the direction of the spin current, and its magnitude reflects the efficiency of converting thermal energy into spin flow.

Studies on single-molecule spin thermoelectric effects have evolved from fundamental theory to material implementations and engineered design strategies. Theoretical work initially focused on SMMs, demonstrating spin-dependent transport under a thermal gradient within the sequential tunneling regime [84]. Owing to intrinsic spin selection rules, spin-up and spin-down electrons can occupy different energy levels and flow in opposite directions. As shown in Fig. 9(a), at a certain molecular energy level ε_0, the spin-up and spin-down currents are nearly equal in magnitude but opposite in direction, resulting in a negligible charge current $I_{ch} = I_\uparrow + I_\downarrow \approx 0$, while the spin current $I_{sp} = I_\uparrow - I_\downarrow$ remains finite. This behavior leads to the natural emergence of a pure spin current, and provides the first theoretical evidence that the spin Seebeck coefficient can exceed its charge counterpart under specific conditions.

Subsequent studies explored the implementation of such effects in real molecular systems. Transition-metal sandwich dimers (MCp_2-Ac-MCp_2, M = Cr, Mn, Fe, and Co) were proposed as promising candidates for molecular spin caloritronics [85]. In gold-molecule-gold junctions, first-principles calculations combined with non-equilibrium Green's function methods revealed that the spin transport is governed by the spin-dependent DOS near the Fermi level. For example, Fig. 9(b) shows that Co-based dimers produce symmetric spin-resolved transmission peaks. Under a temperature gradient, the asymmetry in Fermi–Dirac distributions results in a net flow of hot and cold electrons in opposite spin channels, yielding a pure spin current with near-zero thermovoltage. As shown in Fig. 9(c), the spin current increases with the temperature gradient. In contrast, Cr and Mn dimers exhibit perfect spin filtering and negative differential thermoelectric resistance, while Fe dimers, lacking spin asymmetry, fail to generate pure spin currents. These findings highlight how the electronic configuration of the metal center determines the thermo-spin transport behavior, enabling targeted molecular design.

With growing insights into electronic structure, more engineered molecular systems have been proposed. In particular, bipolar magnetic molecules (BMMs), which possess HOMO and LUMO levels from opposite spin channels, offer a promising platform for controllable SSE [86]. As shown in Fig. 9(d), the HOMO of BMMs is spin-up while the LUMO is spin-down, forming a built-in spin-flip gap. Under a thermal bias, spin-up and spin-down electrons naturally propagate in opposite directions, forming a pure spin current. In specific molecules such as $V^{II}(phen)_2(NCS)_2$, a gate voltage effectively tunes the alignment between the molecular orbitals and the Fermi level. For instance, at the optimized gate voltage shown in Fig. 9(e) (V_G = 0.15 V), the HOMO and LUMO simultaneously approach the Fermi level, leading to nearly equal but oppositely directed spin currents, which cancel charge flow and enhance spin flow. Temperature-dependent results (Fig. 9(f)) show that this pure spin current remains stable across a broad temperature range, indicating robust gate-tunable SSE behavior. In comparison with SMMs and sandwich dimers, BMMs demonstrate

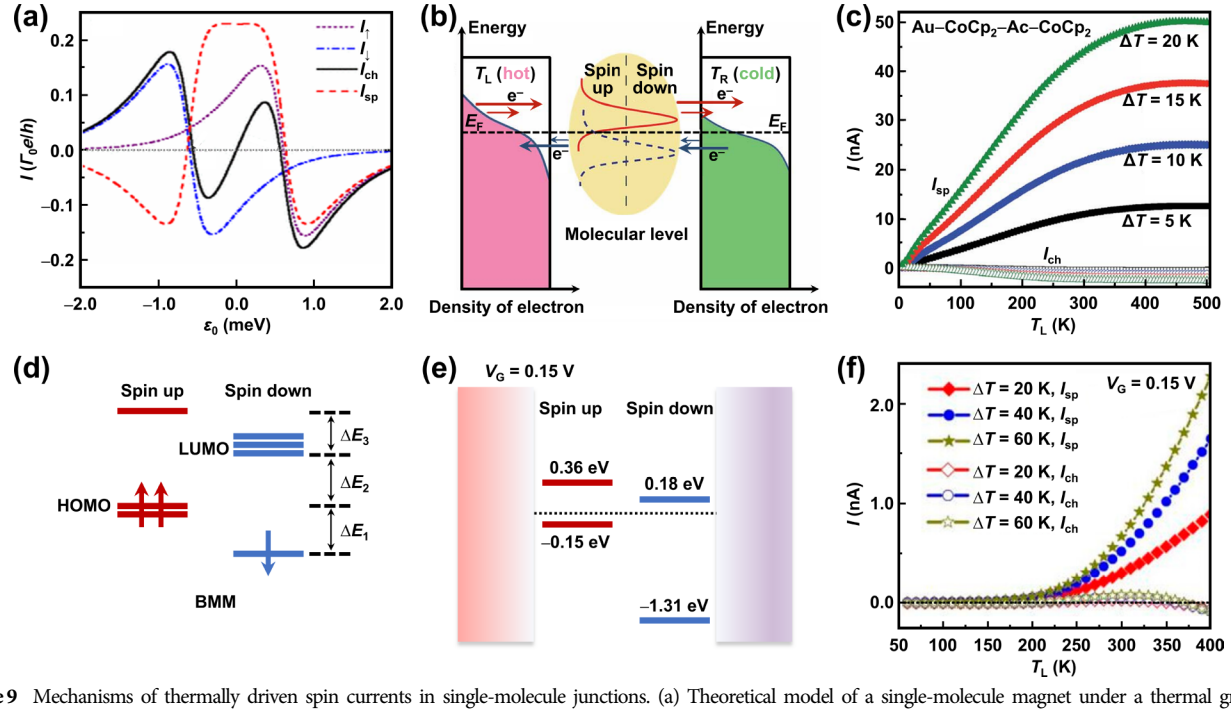

Figure 9 Mechanisms of thermally driven spin currents in single-molecule junctions. (a) Theoretical model of a single-molecule magnet under a thermal gradient, generating a pure spin current. Reproduced with permission from Ref. [84], © The American Physical Society 2010. (b) Spin-resolved transmission spectra for Co-based sandwich dimers, displaying symmetric peaks near the Fermi level. (c) Spin current increasing with the applied thermal gradient. Reproduced with permission from Ref. [85], © The Royal Society of Chemistry 2019. (d) BMM design enabling spin-separated thermal transport. (e) Gate-tuning of molecular orbitals in BMMs for optimized spin current. (f) Robust and gate-tunable SSE across a wide thermal range. Reproduced with permission from Ref. [86], © American Chemical Society 2023.

the advantages of molecular orbital engineering, offering the enhanced flexibility in designing spin caloritronic functionalities.

Taken together, research into single-molecule spin thermoelectric effects has progressed from theoretical models based on SMMs, through chemically diverse transition-metal dimers, to orbital-level control in BMMs. This trajectory outlines a clear strategy spanning mechanism, molecular design, and device integration. These advances not only deepen the understanding of spin-heat coupling at the molecular scale, but also provide a practical foundation for developing energy-efficient and integrable spintronic technologies [87–90].

3.6 Single-molecule spin interface effect

In single-molecule spintronic devices, the interfacial geometry, coupling strength, and energy-level alignment between the molecule and the electrodes critically determine spin-transport properties [91]. The interface not only governs charge injection efficiency, but also fundamentally controls spin injection, spin polarization, and spin coherence. Theoretical studies indicate that even if a molecule possesses extended π-conjugation and supports well-defined spin-polarized states, the expression of these states in a device crucially depends on the symmetry and strength of interfacial coupling [92]. When the coupling is weak or strongly asymmetric, the π orbitals of the molecule do not hybridize efficiently with electrode states, leading to rapid spin dissipation at the interface and a significantly weakened magnetotransport response.

From a design perspective, three interrelated aspects of the molecule–electrode interface are particularly important: anchoring groups, contact geometry, and coupling strength. The chemical nature of the anchoring groups, such as thiols, amines, nitriles, isocyanides, N-heterocyclic carbenes, carboxylates, or π–π contacts to graphitic electrodes, controls both bonding configuration and the degree of orbital hybridization, thereby establishing the foundation for spin injection and spin selectivity. Contact geometry, encompassing binding site (e.g., top, bridge, hollow, and edge versus basal plane), adsorption angle, molecular tilt, and the electrode dimensionality (three-dimensional metal or two-dimensional material), modulates local symmetry, effective overlap, and the spatial distribution of spin density at the interface. Together, these factors determine the effective molecule–electrode coupling strength and the resulting energy-level alignment, which in turn govern whether spin-polarized states are weakly probed in the tunneling regime, strongly broadened into hybrid interface states, or subject to many-body phenomena such as the Kondo effect. Optimizing spintronic performance thus requires a balanced interfacial design: Coupling must be strong enough to achieve efficient spin injection and robust readout, yet not so strong as to quench molecular spin states or accelerate decoherence.

These principles have been experimentally confirmed. As shown in Fig. 10(a), a single-molecule spintronic device was fabricated in which a manganese dibenzotetraaza[14]annulene single-molecule magnet (Fe-Mn(DBTAA)-Fe) is bridged between two ferromagnetic Fe electrodes. By tuning the molecular contact geometry with the electrodes without altering the molecular backbone, the direction and magnitude of spin-polarized transport were both found to change markedly (Fig. 10(b)). Notably, the MR response even exhibited sign reversal under different interfacial configurations [93]. These findings demonstrate that interface-induced reconstruction of electronic states, particularly the overlap between metal d orbitals and ligand orbitals, is a key factor in establishing spin-selective transport channels and in controlling whether a molecular junction exhibits positive or negative MR.

Further investigations reveal that when a molecule possesses strong magnetic anisotropy, interfacial effects can amplify this intrinsic property, enabling stable MR responses even at room temperature. As shown in Fig. 10(c), single-molecule junctions based on Fe-terephthalic acid (TPA) were constructed with controlled electrode geometry and adsorption angle. The corresponding devices exhibited a pronounced angle-dependent anisotropic MR (AMR) effect (Fig. 10(d)) [94]. This highlights the dominant role of the interface in shaping the spatial configuration of molecular spin responses, effectively translating molecular magnetic anisotropy into device-level anisotropic spin transport through controlled contact geometry.

Beyond structural considerations, the chemical composition and electronic structure of the interface also critically influence spin transport. In Fig. 10(e), a study employing $[M^{II}(tzpy)_2(NCSe)_2]$ complexes (M = Co, Mn, and Ni; tzpy = 3-(2-pyridyl)-[1,2,3]triazolo[1,5-a]pyridine; and NCSe = selenocyanate) as molecular bridges between a ferromagnetic Ni tip and a nonmagnetic Au electrode revealed that only the Co^{II} complex exhibited a strong MR signal, whereas the Mn^{II} and Ni^{II} analogues showed negligible variation [95]. This implies that although a finite total spin is necessary, efficient spin-selective coupling occurs only when the symmetry and density of states of the molecular d orbitals match those of the ferromagnetic electrode. Further evidence comes from electrode-comparison experiments: When the same Co complex was connected to Fe, Co, or Au electrodes, only ferromagnetic contacts generated noticeable MR, whereas nonmagnetic Au resulted in negligible spin transport (Fig. 10(f)). These results illustrate that electrodes act not only as reservoirs and spin-polarized sources, but also as spin filters, with effectiveness governed by their intrinsic magnetism and local electronic structure.

Interfacial engineering also enables functional programmability. In some molecular junction systems, reversible switching between conductive and insulating states has been achieved by reconfiguring the molecular contact geometry, thereby inducing controllable transitions between spin states and realizing spin-switching behavior through interface-dependent mechanisms [96]. This extends the role of interface design into a platform for dynamically reconfigurable spintronics, where the same molecule can be switched between distinct spin-transport regimes through mechanical, electrical, or chemical modulation of contacts. In more complex systems, the interface can even dictate the emergence of quantum many-body behaviors. For example, in PTM radical molecules, a strong anticorrelation has been observed between the Kondo resonance and MR: With poor interfacial symmetry, the Kondo resonance is enhanced but spin polarization is weakened; conversely, with more symmetric coupling, MR increases while Kondo features diminish [97]. Remarkably, mechanical stretching of the electrodes enables dynamic switching between these two regimes, offering quantum-level evidence that the interface governs not only the magnitude of spin signals but also the dominant transport mechanism in molecular devices.

To summarize, these examples underscore that interfacial spin effects determine the injection and retention of spin polarization, as well as the response type, stability, and programmability of single-molecule spintronic devices. Practically, the alignment of molecular

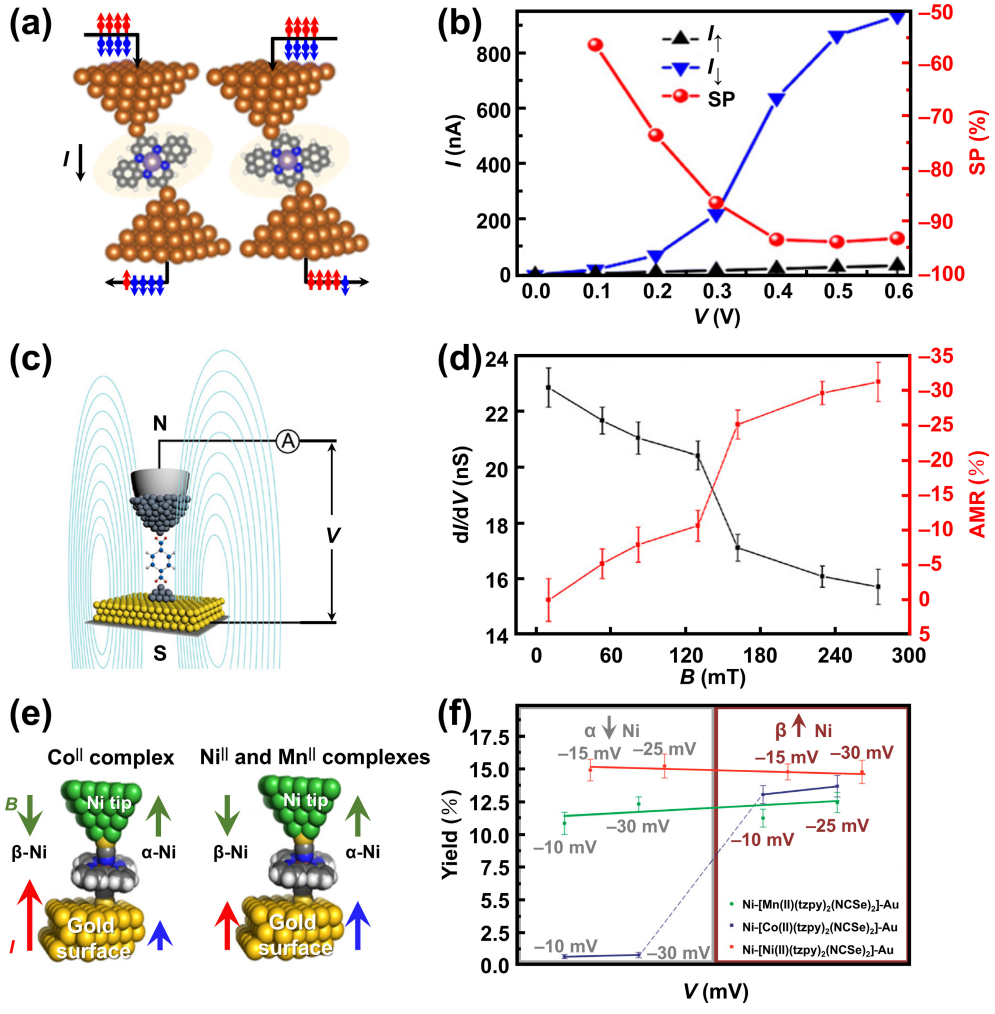

Figure 10 Interfacial control of spin transport in single-molecule spintronic devices. (a) Fe-Mn(DBTAA)-Fe junction with tunable contact geometry. (b) Interfacial geometry altering the magnitude and direction of MR. Reproduced with permission from Ref. [93], © The Royal Society of Chemistry 2022. (c) TPA-Fe junction exhibiting angle-dependent spin transport. (d) Angle-resolved AMR confirming interface-enhanced magnetic anisotropy at room temperature. Reproduced with permission from Ref. [94], © American Chemical Society 2015. (e) Spin transport in [M^{II}(tzpy)$_2$(NCSe)$_2$] (M = Co, Mn, and Ni) complexes showing metal-dependent MR. (f) Electrode-material-dependent MR, showing significant spin filtering only with ferromagnetic contacts. Reproduced with permission from Ref. [95], © American Chemical Society 2017.

orbital density of states with electrode bands, the magnetic compatibility between molecular spins and electrode spin polarization, the geometric configuration and mechanical flexibility of the junction, and the choice of anchoring chemistry converge to form the core regulatory framework of molecular-scale spin devices. Future breakthroughs will therefore rely not only on "designing a good molecule", but also equally on "constructing a controllable interface" in which anchoring groups, contact geometry, and coupling strength are deliberately engineered to maximize spin injection, spin polarization, and spin coherence under realistic operating conditions.

4 Single-molecule spin devices

The diverse and profound spin-related effects observed at the single-molecule scale, which are characterized by strong nonlinearity and exceptional tunability, enable the construction of spintronic devices with clearly defined functionalities. As conventional microelectronics nears its fundamental physical limits, the development of novel device architectures that exploit electron spin, rather than charge, has emerged as a promising strategy to overcome existing bottlenecks in power consumption, scaling, and multifunctionality. Consequently, single-molecule spintronic devices have thus attracted increasing attention, offering unprecedented functional specificity and integration potential at the ultimate limit of miniaturization. These advances are driven by the deepened understanding and precise control of quantum phenomena such as spin-dependent transport, spin relaxation, and magnetic coupling within molecular systems. This chapter focuses on representative device prototypes that utilize these physical effects, including spin valves for data readout and storage, spin switches for logic control, and single-molecule spin qubits for quantum computing applications. Particular emphasis is placed on elucidating how microscopic spin phenomena can be effectively converted into macroscopic device functionalities.

4.1 Single-molecule spin valve (SMSV)

SMSVs represent the atomic-scale embodiment of classical spin-valve mechanisms, wherein a single molecule acts as a tunneling barrier between two ferromagnetic electrodes [98]. By switching the

relative magnetization alignment of the electrodes, between parallel (P) and antiparallel (AP) configurations, a significant contrast in spin-selective electron transmission is achieved, resulting in distinct conductance states. The device performance is typically quantified by the following equation [99]

$$\mathrm{MR} = \frac{R_{\mathrm{AP}} - R_{\mathrm{P}}}{R_{\mathrm{P}}} \tag{7}$$

which reflects the spin filtering efficiency under varying molecular configurations and bias conditions.

In such devices (Fig. 11(a)), under the P configuration, the majority-spin states of both electrodes align near the Fermi level, enhancing molecular coupling and transmission for majority spins, thus yielding a low-resistance state. Conversely, in the AP configuration, this alignment is disrupted, leading to asymmetric coupling across spin channels and suppression of the dominant transmission pathway, thereby switching the system into a high-resistance state. This switching behavior leads to a characteristic hysteresis in current–voltage responses [99].

Unlike conventional spintronic structures, SMSVs exhibit fundamentally different origins of magnetism: Electrode spin polarization arises from exchange-split band structures, whereas molecular magnetism may result from spin-selective orbital hybridization (e.g., in H_2Pc) or from intrinsic magnetically anisotropic spins in SMMs (e.g., Fe_4 and $TbPc_2$). Their coupling involves DOS alignment, super exchange interactions, and molecular orbital symmetry, all of which govern spin transport efficiency [98, 100].

Theoretical predictions using Ni-BDT-Ni (BDT = 1,4-benzenedithiolate) junctions first suggested that spin-valve effects could occur at the molecular level, with transmission differing by orders of magnitude between P and AP configurations [98]. Subsequent first-principles simulations confirmed this behavior. For example, Fig. 11(b) illustrates a Ni-BDT-Ni device with Au electrodes. Although its ground state favors AP alignment, an external magnetic field can switch the system to the P state, yielding a sharp conductance increase (MR ≈ 53%). Replacing Ni with Mn alters the dominant spin channel and suppresses MR, highlighting the critical influence of electrode–molecule hybridization on spin filtering [100].

Experimentally, such interface hybridization effects were verified in Co–H_2Pc–Co junctions. Using spin-polarized STM (SP-STM), researchers bridged a single H_2Pc molecule between a Co tip and a Co island (Fig. 11(c)). The junction exhibited high conductance (G_0 of ~ 0.26) and strong MR (~ 60%), even at a low areal resistance product. The LUMO strongly hybridizes with minority-spin states and weakly with majority-spin states, making the P configuration favorable for minority-spin transport. In contrast, the AP state suppresses transmission due to asymmetric spectral broadening. This phenomenon can be accurately described by the Breit–Wigner resonance model, which indicates the crucial role of energy level alignment and interfacial symmetry [101].

When a molecule possesses intrinsic magnetism and pronounced magnetic anisotropy, it can host bistable spin states protected by an anisotropy barrier, thereby enabling spin-selective transport and switching at the molecular scale. In junctions where such magnetic molecules are coupled to ferromagnetic electrodes, the spin-valve response is dictated by the interplay between the electrode spin polarization and the molecules' bistable spin orientations. For example, Fig. 11(d) shows a junction incorporating SMMs, in which an external magnetic field or an

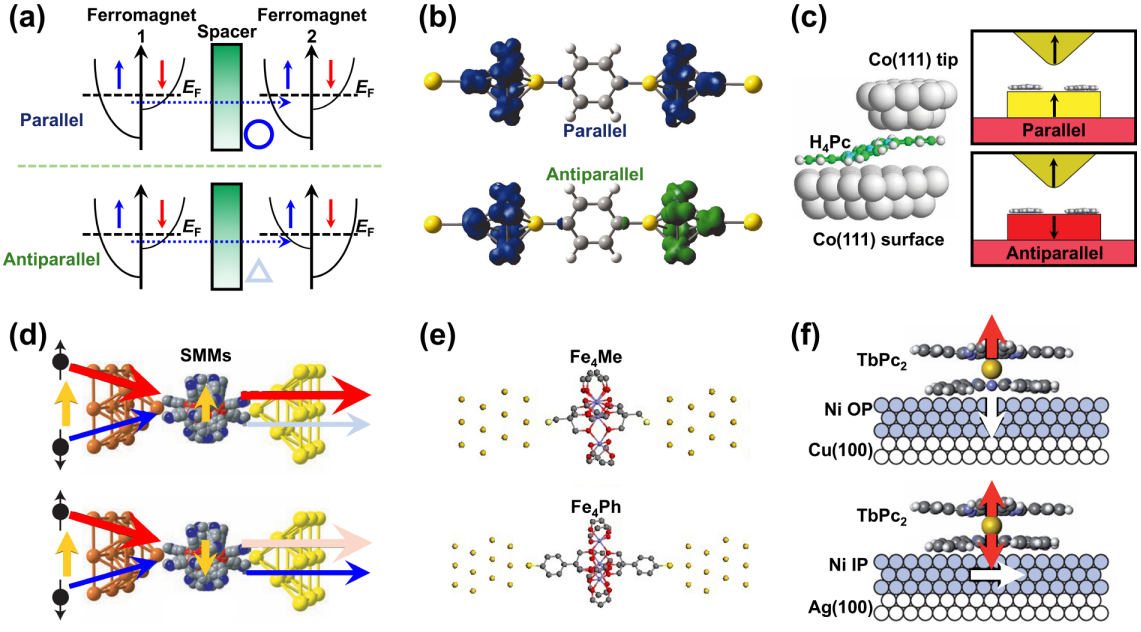

Figure 11 Spin-valve behaviors in single-molecule junctions. (a) Schematic of a single-molecule spin valve with conductance dependent on electrode magnetization alignment. Reproduced with permission from Ref. [99], © Elsevier B.V. 2011. (b) Theoretical simulation showing large magnetoresistance in a Ni-BDT-Ni junction and the magnetoresistance's sensitivity to electrode–molecule coupling. Reproduced with permission from Ref. [100], © American Physical Society 2003. (c) SP-STM measurements revealing high magnetoresistance in Co–H_2Pc–Co junctions via LUMO-spin hybridization. Reproduced with permission from Ref. [101], © Springer Nature Limited 2011. (d) SMM-based spin-valve junction with a magnetic source electrode and a diamagnetic drain electrode, illustrating spin-dependent transmission under parallel and antiparallel alignment. Reproduced with permission from Ref. [3], © Springer Nature Limited 1969. (e) Ligand-engineered spin filtering in Au-Fe_4-Au junctions, showing enhanced magnetoresistance with phenyl ligands. Reproduced with permission from Ref. [102], © Zu, F. X. et al. 2014. (f) Interfacial doping in $TbPc_2$/Ni systems, improving spin retention and thermal stability via tuned superexchange. Reproduced with permission from Ref. [103], © American Physical Society 2011.

applied bias can shift molecular levels to open or block spin-flip pathways, toggling the junction between high- and low-conductance states [3]. Depending on the coupling strength, additional effects such as Coulomb blockade, Kondo resonances, or vibronic contributions may further modulate this spin-switching behavior. Importantly, spin filtering can also be realized without magnetic electrodes when transport is governed primarily by the molecules' intrinsic spin structure. In an Au-Fe_4-Au junction with non-magnetic electrodes (Fig. 11(e)), ligand modifications lead to markedly different spin transport: methyl ligands localize spin density near the Fe core, enabling near-perfect spin filtering, whereas phenyl ligands introduce π-bridge-induced asymmetry that dramatically enhances the MR, reaching up to 1800% [102].

Moreover, interfacial engineering offers a tunable pathway to tailor spin valve functionality. As illustrated in Fig. 11(f), adsorbing $TbPc_2$ on an anisotropic Ni surface and doping with oxygen or lithium modifies the interfacial super exchange interaction. This enables precise control over molecular magnetization, improves thermal stability, and helps retain spin state under ambient conditions [103].

It is worth noting that the performance of SMSVs is governed by several key factors:

(1) Energy level alignment and spectral broadening symmetry, which affect the efficiency of spin transmission and can be tuned via gate voltage or molecular design [99–102].

(2) Electrode spin polarization, which determines the magnitude and type of spin injection [100, 101].

(3) Molecular spin states, particularly in SMMs, which enable spin switching even with non-magnetic contacts [3, 102].

(4) Interface properties, including π-bridge ligands, chemical doping, and super exchange interactions, which affect spin coupling and operational stability [101–103].

(5) Contact regime, where the transition from tunneling to direct contact modulates both conductance and MR behavior [101].

Building on these foundations, recent advances demonstrate that SMSVs can further exploit interface-engineered spin injection to access functionalities beyond conventional MR readout. In a graphene-based SMSV incorporating a ferromagnetic Ni/Al_2O_3 electrode, a maleimide-functionalized molecular bridge was covalently connected between graphene point contacts [104]. In this system, the interfacial spin polarization and molecular asymmetry jointly convert molecular chirality into a magnetization-dependent transport signal via the CISS effect. Continuous current–time measurements enabled real-time identification of reaction intermediates and in situ monitoring of chirality evolution during a Michael addition, highlighting how carefully designed electrode–molecule interfaces extend SMSVs toward dynamic chemical and stereochemical sensing at the single-molecule level.

With atomic-scale architecture, tunable magnetic functionality, and multiple degrees of freedom, SMSVs serve as ideal testbeds for investigating spin-selective transport and engineering functional spintronic devices. Although challenges remain in stability, reproducibility, and operational temperature, ongoing progress in interface design, molecular synthesis, and device integration continues to advance SMSVs towards practical applications.

4.2 Single-molecule spin switch

Single-molecule spin switches are nanoscale systems in which the spin state of an individual molecule is reversibly modulated by external stimuli, leading to significant changes in electrical conductance [105]. The underlying mechanism arises from the strong coupling between the molecular spin degree of freedom and the electronic transport channel. Typically, a molecule is bridged between two electrodes, and when subjected to stimuli such as electric or magnetic fields, chemical ligands, light, or mechanical force, its spin-resolved energy levels undergo reconfiguration. This alters either the orbital alignment with the Fermi levels of the electrode or the spin-dependent scattering behavior, resulting in distinct "on" and "off" conductance states.

A widely studied model system is FePc, employed to investigate how external fields regulate orbital configuration and spin transport. As shown in Fig. 12(a), FePc adsorbed on an Au(111) surface can be probed by STM to form a tip-FePc-Au tunnel junction. Upon applying a perpendicular magnetic field, the magnetic moment orientation of the Fe center changes, promoting hybridization between its d_{z^2} and d_π orbitals. This switches the dominant transport channel, experimentally observed as a transition from a dip to a peak in the dI/dV spectra under cryogenic conditions (Fig. 12(b)) [106]. Theoretical calculations support this orbital-mixing mechanism, corresponding to a field-tunable AMR effect. In another approach using superconducting Nb tips, researchers demonstrated reversible switching of the Kondo resonance by modulating the tip–molecule distance, effectively tuning the tunneling coupling strength [107].

Metallocene-type molecules such as nickelocene have also been used as spin-switching platforms owing to their high chemical stability. When adsorbed on Cu(111), voltage pulses trigger transitions between a magnetic S = 1/2 state and a non-magnetic S = 0 state. These transitions manifest as the appearance and disappearance of a Kondo resonance in dI/dV spectra. The switching behavior is attributed to charge distribution at the metal-molecule interface and changes in vibrational coupling, as supported by theoretical simulations [108].

In addition to physical stimuli, chemical ligand coordination provides an alternative route for spin state control. For example, in Co^{II} tetraphenylporphyrin (CoTPP) molecules assembled on Au(111), the adsorption of weak axial ligands such as NH_3 or NO induces a transition from an LS (S = 0) to an HS state (S = 1/2 or 1). The HS state is identified by the emergence of Kondo or zero-bias peaks in STM measurements (Fig. 12(c)), and the process is reversible via thermal treatment or ligand desorption (Fig. 12(d)) [109]. This switching arises from ligand-induced changes in crystal field symmetry, reorganizing d-orbital occupancy.

To enable operation under ambient conditions, electrode-bridged single-molecule junctions have been developed. For instance, in an Au-CoTPP-Au configuration, the introduction of 4-pyridinethiol ligands induces a spin transition by altering the coordination geometry of the Co center from planar (S = 0) to pyramidal (S = 1). As shown in Figs. 12(e) and 12(f), this structural transformation leads to clear conductance switching, demonstrating room-temperature spin control [110].

Currently, research on single-molecule spin switches has evolved from external physical field manipulation to internal molecular design and chemical responsiveness. Despite variations in stimuli and detection methods, these systems consistently exhibit strong coupling among molecular structure, spin states, and transport properties. Key challenges for practical applications include improving energy efficiency, switching speed, and operational stability under ambient conditions. These advances lay the groundwork for spin-based logic and memory at the molecular scale [108, 111, 112].

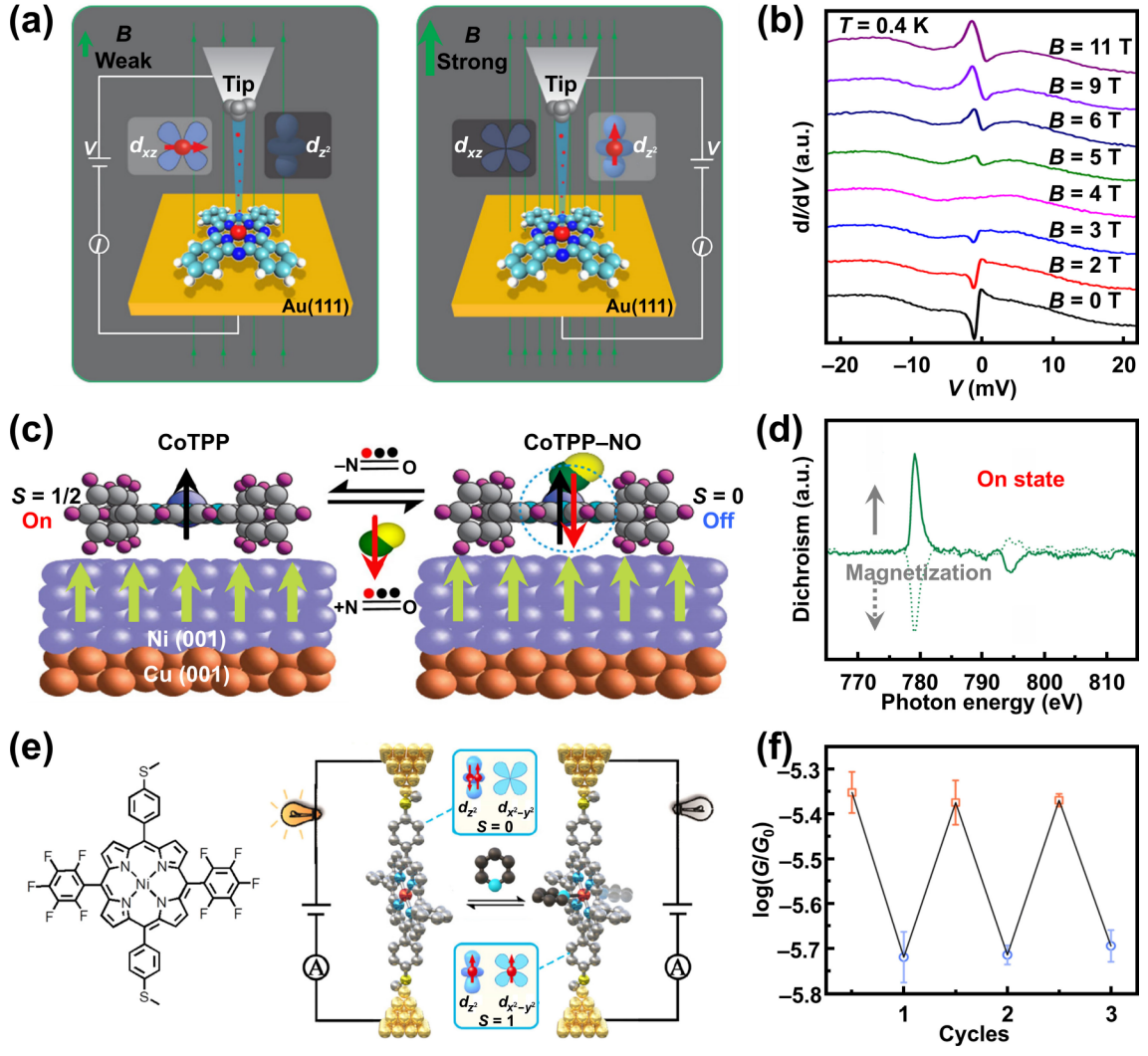

Figure 12 Mechanisms and control of spin switching in single-molecule junctions. (a) STM configuration of FePc on Au(111) for studying spin-orbital reconfiguration under magnetic fields. (b) Field-induced orbital switching transport from a conductance dip to a peak. Reproduced with permission from Ref. [106], © Yang, K. et al. 2019. (c) Spin state transition in CoTPP triggered by axial ligand coordination (e.g., NH_3), generating Kondo signatures. (d) Reversible spin switching via thermal ligand dissociation. Reproduced with permission from Ref. [109], © Macmillan Publishers Limited 2010. (e) Coordination-induced geometry conversion from planar (S = 0) to pyramidal (S = 1) in a CoTPP junction. (f) Room-temperature conductance switching driven by chemical coordination. Reproduced with permission from Ref. [110], © Chinese Chemical Society 2021.

4.3 Single-molecule spin qubits

Spin qubits represent a physical realization of quantum information processing, using the spin state of a single electron (or hole) as the information carrier [113]. Unlike classical bits, which are confined to distinct "0" or "1" states, spin qubits can exist in arbitrary superpositions of these basis states and leverage quantum entanglement to enable parallel computation. As a result, they have emerged as promising candidates for applications in quantum computing, sensing, communication, and fundamental physics [114, 115]. A single-molecule spin qubit is a molecular-scale realization wherein the electronic spin of an individual molecule serves as the basic unit of quantum information. This approach benefits from intrinsic molecular uniformity, high chemical tunability, precise structural control at the nanoscale, and diverse spin configurations, thereby offering a bottom-up chemical platform to address key challenges in scalability, coherence, and controllable interqubit coupling within large-scale quantum architectures.

Current research on single-molecule spin qubits primarily focuses on paramagnetic metal complexes, organic radicals, and polynuclear molecular clusters. To manipulate and detect spin states at the single-molecule level, these systems are typically integrated into solid-state devices where external electric or magnetic fields enable spin initialization and control. High-precision measurement techniques are then employed to characterize quantum properties such as spin relaxation and coherence time. Representative device configurations include molecular junctions, STM-based setups, and hybrid systems coupled to microwave resonators.

For instance, combining atomic force microscopy (AFM) with ESR allows for spectroscopic resolution of molecular spin states. As shown in Fig. 13(a), pentacene molecules adsorbed on a gold microstrip and insulated by a thick NaCl layer suppress unwanted tunneling. By applying a gate voltage to modulate single-electron tunneling between the molecule and the AFM tip, spin triplet states were resolved with sub-meV energy resolution at 8 K, with

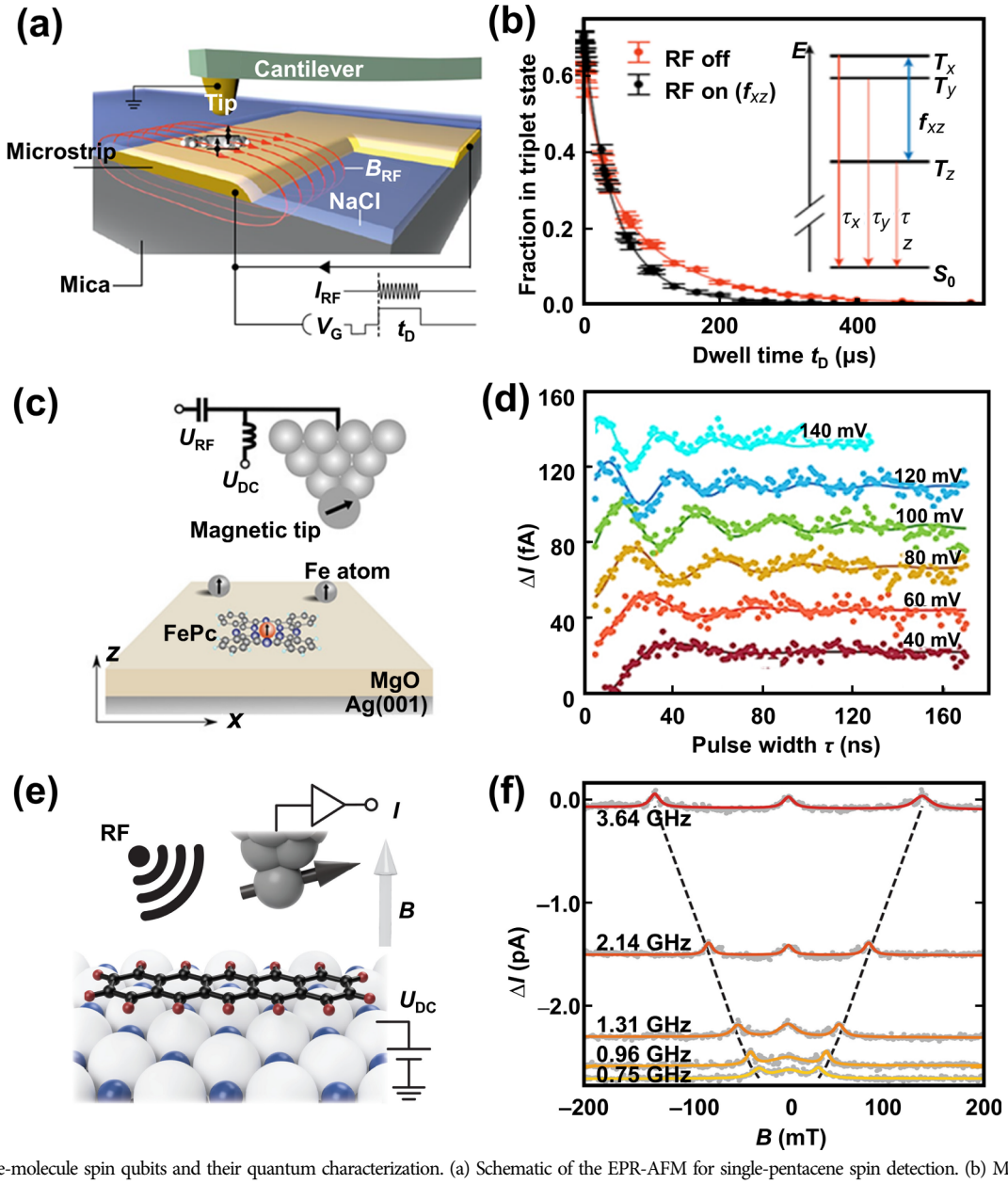

Figure 13 Single-molecule spin qubits and their quantum characterization. (a) Schematic of the EPR-AFM for single-pentacene spin detection. (b) Molecular excited-state decay without (red) and with (black) a broadband RF pulse. Reproduced with permission from Ref. [116], © Sellies, L. et al. 2023. (c) EPR-STM setup for detecting spin transitions in a single FePc molecule. (d) Rabi oscillations measured as ΔI versus pulse duration at different RF voltages. Reproduced with permission from Ref. [117], © Willke, P. et al. 2021. (e) EPR-STM junction for probing single-pentacene spin dynamics. (f) EPR spectra acquired as a function of magnetic field at different frequencies. Reproduced with permission from Ref. [114], © Kovarik, S. et al. 2024.

observed spin coherence time on the order of microseconds (Fig. 13(b)) [116].

Alternatively, FePc molecules studied via STM-ESR junctions demonstrate coherent spin control through radio frequency (RF) excitation (Fig. 13(c)). RF voltage pulses drive spin transitions between spin ground and excited states, while pulse sequences such as those used in Rabi oscillations and Hahn echo measurements reveal spin coherence dynamics (Fig. 13(d)). Moreover, spin-polarized RF currents have been employed to coherently manipulate individual spins, while spin-polarized direct current (DC) induces incoherent spin flips by altering the spin expectation value [117].

Further advances have been achieved using electron paramagnetic resonance-STM (EPR-STM) (Fig. 13(e)). At 4.5 K, a spin-polarized RF current was injected into a pentacene molecule adsorbed on an MgO/Ag(001) substrate via a magnetic STM tip. The system, hosting an unpaired electron (S = 1/2) across the SOMO and singly unoccupied molecular orbital (SUMO), serves as an ideal quantum dot model. Spin dynamics were monitored by modulations of the tunneling current (ΔI), and lock-in amplification was used to analyze EPR signal line shapes and bias dependence (Fig. 13(f)) [114].

Achieving high-performance single-molecule spin qubits requires not only advanced measurement techniques, but also rational molecular design. Through careful selection of ligands, metal centers, and molecular backbone topology, it is possible to fine-tune spin energy levels, spin-orbit coupling, and environmental decoherence, thereby extending coherence time and improving

quantum gate fidelity. Certain systems, such as endohedral metallofullerenes or multinuclear complexes, inherently support multiple qubits and higher-dimensional Hilbert spaces, offering prospects for parallel quantum operations across multiple spin degrees of freedom [118–121].

Therefore, the development of single-molecule spin qubit devices depends not only on the intrinsic molecular quantum properties, but also on the holistic optimization of external control fields, quantum tunneling regimes, and device architecture. Through coordinated engineering of both internal and external parameters, it becomes possible to enhance quantum information storage and manipulation, thereby paving the way for molecular spin-based quantum technologies [122].

5 Conclusions and prospects

This review provides an overview of spin-active molecular systems, encompassing discrete spin centers and spin-polarizable scaffolds, and their integration into electrically addressable junction platforms to probe and control spin at the single-molecule level. Representative molecular building blocks include SMMs, SCO complexes, open-shell organic radicals, and chiral frameworks, while commonly employed platforms span MCBJ, electromigrated nanogaps, scanning-probe junctions, and three-terminal gated geometries. Across these systems, experimental studies have enabled the resolution of energy-level alignment and occupancy control, the observation of Kondo features exhibiting Zeeman and exchange splitting, the detection of AMR and spin-dependent thermoelectric responses, and the implementation of prototype spin-valve, spin-filter, and spin-switch functionalities. Collectively, these advances outline design principles for achieving low-energy switching and programmable spin functionalities at the molecular scale. At present, single-molecule spin memory and logic devices are primarily regarded as quantitative testbeds for benchmarking readout contrast, retention, and gate controllability under comparable conditions, rather than as immediately deployable technologies.

Despite considerable progress, practical deployment remains constrained by device-to-device variability, limited stability near room temperature, and challenges in cross-platform comparison. Fluctuations in binding geometry, local fields, vibronic coupling, and electrode morphology introduce substantial uncertainty into spin readout and control. In the near term, systematic strategies for improving reproducibility are expected to be particularly impactful. These include large-scale statistical measurements across thousands of junction realizations, the use of well-defined reference molecules on the same chip or within the same experimental campaign, and standardized control experiments that deliberately vary only one parameter at a time, such as anchor chemistry, electrode materials, or temperature window. Automated data acquisition, coupled with transparent statistical analysis capable of distinguishing intrinsic molecular behavior from rare high-conductance outliers or unstable configurations, will be essential for establishing robust distributions of spin-dependent observables. In parallel, unified performance metrics, such as barrier heights and retention for memory devices, switching thresholds and energy per operation for logic or switching devices, on/off ratio and signal-to-noise ratio, and cycling endurance, need to be consolidated and routinely reported to enable meaningful cross-platform comparison.

One priority lies in advancing molecular systems. Ideal candidates should integrate intrinsic spin functionality with interfacial robustness and synthetic modularity. For discrete spin centers, large magnetic anisotropy and high-spin ground states that resist rapid spin-phonon relaxation are desirable, especially if such anisotropy can be preserved up to or near room temperature. SCO complexes should exhibit thermally addressable bistability with measurable hysteresis under near-ambient conditions, allowing modest thermal or electrical stimuli to toggle spin states without sacrificing retention. Organic radicals must maintain chemical persistence and spin polarization under operating bias and elevated temperatures, while chiral scaffolds require well-defined stereochemical series with tunable helical pitch to enable rigorous quantification of CISS effect across broad temperature ranges. Across all categories, rigid π-conjugated backbones help suppress low-frequency torsions and mitigate thermally activated conformational noise, while anchor groups compatible with metal or two-dimensional electrodes (e.g., thiols, nitriles, isocyanides, N-heterocyclic carbenes, or polyaromatic π–π contacts) improve geometric stability and electronic coupling. Where applicable, incorporation of redox-, photo-, or proton-responsive units provides orthogonal control over spin states, and isotopic or nuclear-spin engineering can help mitigate decoherence. To strengthen the practical perspective, future studies should explicitly correlate key molecular descriptors, such as spin ground state, zero-field splitting or anisotropy, redox potentials, and vibrational signatures, with device-level metrics, including spin polarization, readout contrast, retention, noise floor, and statistical yield. This approach will enable reproducible and quantitative comparisons under standardized bias, temperature, and magnetic field conditions.

A second key direction involves elucidating spin-transport mechanisms at the molecular scale. The interplay among symmetry, exchange interactions, and spin-orbit coupling warrants systematic investigation, with particular attention to selection rules governing spin-polarized transport and their spectroscopic signatures. The chiral-induced spin selectivity effect should be assessed using well-controlled stereochemical series alongside achiral reference systems, enabling separation of genuine spin filtering from contributions due to electrode asymmetry, inelastic scattering, or local heating. Spin-phonon coupling and nonequilibrium thermo-spin phenomena call for combined frequency- and time-domain probes to quantitatively extract relaxation and dephasing pathways. Understanding how these processes evolve from cryogenic to intermediate and ultimately to room-temperature regimes is crucial for realistic device operation. Where feasible, parameter estimates should be anchored by *ab initio* transport calculations that incorporate realistic interfaces and vibrational couplings, and should be validated against temperature- and field-dependent measurements. Such tightly integrated experimental and theoretical efforts will be central to determining which spin effects can survive at technologically relevant temperatures and under device-level noise conditions.

Another critical area concerns device architecture. Low-noise interfaces utilizing two-dimensional electrodes and molecularly defined van der Waals gaps can improve geometrical reproducibility, reduce background trap states, and enhance thermal and environmental stability. Robust anchoring groups and conformationally rigid molecular backbones help minimize drift and suppress thermally driven configurational changes, while encapsulation layers or dielectric overlayers can screen charge noise

and protect against chemical degradation under ambient operation. Three-terminal control, coupled with time-resolved readout, facilitates standardized measurement protocols across laboratories and provides a natural route toward circuit integration. For spin-based quantum applications, isotopic purification, clock-transition engineering, and rigid ligand environments may extend coherence time, whereas careful thermal engineering of substrates and local phonon environments will be required to retain quantum coherence above cryogenic temperatures. Electron spin resonance or optically detected magnetic resonance can provide non-invasive, high-fidelity spin readout, and weak coupling to microwave or optical cavities could enable coherent interfaces to photons. Designed molecular arrays, integrated with patterned electrodes or on-chip resonators, can serve as testbeds for controllable spin-spin coupling, elementary error-mitigation schemes, and basic quantum-gate operations.

Looking ahead, the development trajectory for single-molecule spintronic devices is likely to proceed in stages. In the near term, the emphasis will remain on statistically robust characterization, improved reproducibility, and demonstrations of selected spin functionalities at elevated (though not yet fully ambient) temperatures on well-controlled platforms. Over the longer term, the key challenges will shift toward achieving room-temperature operation, wafer-scale fabrication of spin-addressable molecular arrays, and seamless integration with complementary metal-oxide-semiconductor (CMOS) or photonic architectures. Progress along these fronts will depend on coordinated advances in molecular design, interfacial engineering, and quantum-coherent control. Through such efforts, single-molecule spin devices may evolve from precision testbeds into functional building blocks for low-power spin logic, on-chip spin sensing, and chemically defined quantum information technologies.

Data availability

Not applicable.

Acknowledgements

This work was financially supported by the National Key R&D Program of China (Nos. 2024YFA1208100, 2021YFA1200102, 2021YFA1200101, and 2023YFF1205803), the National Natural Science Foundation of China (Nos. 22595390 and 22173050), Beijing National Laboratory for Molecular Sciences (No. BNLMS-CXXM-202407), and Fundamental and Interdisciplinary Disciplines Breakthrough Plan of the Ministry of Education of China (No. JYB2025XDXM404).

Declaration of competing interest

All the contributing authors report no conflict of interests in this work.

Author contribution statement

Y. Z. Z. and W. S.: Investigation, literature collection, formal analysis, and writing – original draft. X. K. H., Q. H. G., C. Z., and R. Z. L.: Data curation and formal analysis. J. G. and M. L. L.: Supervision, and writing – review & editing. C. C. J. and X. F. G.: Conceptualization, supervision, project administration, and funding acquisition. All the authors have approved the final manuscript.

Use of AI statement

None.

References

[1] Fahrendorf, S.; Atodiresei, N.; Besson, C.; Caciuc, V.; Matthes, F.; Blügel, S.; Kögerler, P.; Bürgler, D. E.; Schneider, C. M. Accessing 4f-states in single-molecule spintronics. *Nat. Commun.* **2013**, *4*, 2425.

[2] Sanvito, S. Molecular spintronics. *Chem. Soc. Rev.* **2011**, *40*, 3336–3355.

[3] Bogani, L.; Wernsdorfer, W. Molecular spintronics using single-molecule magnets. *Nat. Mater.* **2008**, *7*, 179–186.

[4] Xin, N.; Guan, J. X.; Zhou, C. G.; Chen, X. J. N.; Gu, C. H.; Li, Y.; Ratner, M. A.; Nitzan, A.; Stoddart, J. F.; Guo, X. F. Concepts in the design and engineering of single-molecule electronic devices. *Nat. Rev. Phys.* **2019**, *1*, 211–230.

[5] Slota, M.; Bogani, L. Combining molecular spintronics with electron paramagnetic resonance: The path towards single-molecule pulsed spin spectroscopy. *Appl. Magn. Reson.* **2020**, *51*, 1357–1409.

[6] Huang, W. T.; Au-Yeung, K. H.; Greule, P.; Stark, M.; Sürgers, C.; Wernsdorfer, W.; Robles, R.; Lorente, N.; Willke, P. An electrically controlled single-molecule spin switch. *Nat. Commun.* **2025**, *16*, 8242.

[7] Heinrich, B. W.; Ehlert, C.; Hatter, N.; Braun, L.; Lotze, C.; Saalfrank, P.; Franke, K. J. Control of oxidation and spin state in a single-molecule junction. *ACS Nano* **2018**, *12*, 3172–3177.

[8] Gehring, P.; Thijssen, J. M.; van der Zant, H. S. J. Single-molecule quantum-transport phenomena in break junctions. *Nat. Rev. Phys.* **2019**, *1*, 381–396.

[9] Morita, T.; Damjanović, M.; Katoh, K.; Kitagawa, Y.; Yasuda, N.; Lan, Y. H.; Wernsdorfer, W.; Breedlove, B. K.; Enders, M.; Yamashita, M. Comparison of the magnetic anisotropy and spin relaxation phenomenon of dinuclear terbium(III) phthalocyaninato single-molecule magnets using the geometric spin arrangement. *J. Am. Chem. Soc.* **2018**, *140*, 2995–3007.

[10] Bairagi, K.; Bellec, A.; Fourmental, C.; Iasco, O.; Lagoute, J.; Chacon, C.; Girard, Y.; Rousset, S.; Choueikani, F.; Otero, E. et al. Temperature-, light-, and soft X-ray-induced spin crossover in a single layer of Fe^{II}-pyrazolylborate molecules in direct contact with gold. *J. Phys. Chem. C* **2018**, *122*, 727–731.

[11] Gee, A.; Jaafar, A. H.; Brachňaková, B.; Massey, J.; Marrows, C. H.; Šalitroš, I.; Kemp, N. T. Multilevel resistance switching and enhanced spin transition temperature in single- and double-molecule spin crossover nanogap devices. *J. Phys. Chem. C* **2020**, *124*, 13393–13399.

[12] Klinduhov, N.; Boukheddaden, K. Vibronic theory of ultrafast intersystem crossing dynamics in a single spin-crossover molecule at finite temperature beyond the born-oppenheimer approximation. *J. Phys. Chem. Lett.* **2016**, *7*, 722–727.

[13] Gütlich, P.; Ksenofontov, V.; Gaspar, A. B. Pressure effect studies on spin crossover systems. *Coord. Chem. Rev.* **2005**, *249*, 1811–1829.

[14] Estrader, M.; Uber, J. S.; Barrios, L. A.; Garcia, J.; Lloyd-Williams, P.; Roubeau, O.; Teat, S. J.; Aromí, G. A magneto-optical molecular device: Interplay of spin crossover, luminescence, photomagnetism, and photochromism. *Angew. Chem., Int. Ed.* **2017**, *56*, 15622–15627.

[15] Meded, V.; Bagrets, A.; Fink, K.; Chandrasekar, R.; Ruben, M.; Evers, F.; Bernand-Mantel, A.; Seldenthuis, J. S.; Beukman, A.; van der Zant, H. S. J. Electrical control over the Fe(II) spin crossover in a single molecule: Theory and experiment. *Phys. Rev. B* **2011**, *83*, 245415.

[16] Aragonès, A. C.; Varese, M.; Garg, K.; Kuang, W. Z.; Wang, Q. K.; Giralt, E.; Mujica, V.; Gutierrez, R.; Cuniberti, G.; Puerta, L. et al. Dipole-induced inversion of spin-dependent charge transport through

α-helical peptide-based single-molecule junctions. *J. Am. Chem. Soc.* **2025**, *147*, 36453–36463.

[17] Ghosh, S.; Mishra, S.; Avigad, E.; Bloom, B. P.; Baczewski, L. T.; Yochelis, S.; Paltiel, Y.; Naaman, R.; Waldeck, D. H. Effect of chiral molecules on the electron's spin wavefunction at interfaces. *J. Phys. Chem. Lett.* **2020**, *11*, 1550–1557.

[18] Naaman, R.; Paltiel, Y.; Waldeck, D. H. Chiral molecules and the electron spin. *Nat. Rev. Chem.* **2019**, *3*, 250–260.

[19] Perrin, M. L.; Burzurí, E.; van der Zant, H. S. J. Single-molecule transistors. *Chem. Soc. Rev.* **2015**, *44*, 902–919.

[20] Nichols, R. J.; Higgins, S. J. Single molecule nanoelectrochemistry in electrical junctions. *Acc. Chem. Res.* **2016**, *49*, 2640–2648.

[21] Kaun, C. C.; Chen, Y. C. Thermoelectric charge and spin current generation in magnetic single-molecule junctions: First-principles calculations. *J. Phys. Chem. C* **2018**, *122*, 12185–12192.

[22] Rabelo, R.; Toma, L. M.; Bentama, A.; Stiriba, S. E.; Ruiz-García, R.; Cano, J. Exploring spin-crossover cobalt(II) single-ion magnets as multifunctional and multiresponsive magnetic devices: Advancements and prospects in molecular spintronics and quantum computing technologies. *Magnetochemistry* **2024**, *10*, 107.

[23] Verlhac, B.; Bachellier, N.; Garnier, L.; Ormaza, M.; Abufager, P.; Robles, R.; Bocquet, M. L.; Ternes, M.; Lorente, N.; Limot, L. Atomic-scale spin sensing with a single molecule at the apex of a scanning tunneling microscope. *Science* **2019**, *366*, 623–627.

[24] Coronado, E. Molecular magnetism: From chemical design to spin control in molecules, materials and devices. *Nat. Rev. Mater.* **2020**, *5*, 87–104.

[25] Cucinotta, G.; Poggini, L.; Pedrini, A.; Bertani, F.; Cristiani, N.; Torelli, M.; Graziosi, P.; Cimatti, I.; Cortigiani, B.; Otero, E. et al. Tuning of a vertical spin valve with a monolayer of single molecule magnets. *Adv. Funct. Mater.* **2017**, *27*, 1703600.

[26] Rinehart, J. D.; Fang, M.; Evans, W. J.; Long, J. R. Strong exchange and magnetic blocking in N_2^{3-}-radical-bridged lanthanide complexes. *Nat. Chem.* **2011**, *3*, 538–542.

[27] Watanabe, A.; Yamashita, A.; Nakano, M.; Yamamura, T.; Kajiwara, T. Multi-path magnetic relaxation of mono-dysprosium(III) single-molecule magnet with extremely high barrier. *Chem.—Eur. J.* **2011**, *17*, 7428–7432.

[28] Mannini, M.; Pineider, F.; Sainctavit, P.; Danieli, C.; Otero, E.; Sciancalepore, C.; Talarico, A. M.; Arrio, M. A.; Cornia, A.; Gatteschi, D. et al. Magnetic memory of a single-molecule quantum magnet wired to a gold surface. *Nat. Mater.* **2009**, *8*, 194–197.

[29] Paschke, F.; Erler, P.; Enenkel, V.; Gragnaniello, L.; Fonin, M. Bulk-like magnetic signature of individual Fe_4H molecular magnets on graphene. *ACS Nano* **2019**, *13*, 780–785.

[30] Miyamachi, T.; Gruber, M.; Davesne, V.; Bowen, M.; Boukari, S.; Joly, L.; Scheurer, F.; Rogez, G.; Yamada, T. K.; Ohresser, P. et al. Robust spin crossover and memristance across a single molecule. *Nat. Commun.* **2012**, *3*, 938.

[31] Lemke, H. T.; Kjær, K. S.; Hartsock, R.; van Driel, T. B.; Chollet, M.; Glownia, J. M.; Song, S.; Zhu, D. L.; Pace, E.; Matar, S. F. et al. Coherent structural trapping through wave packet dispersion during photoinduced spin state switching. *Nat. Commun.* **2017**, *8*, 15342.

[32] Kuppusamy, S. K.; Mizuno, A.; García-Fuente, A.; van der Poel, S.; Heinrich, B.; Ferrer, J.; van der Zant, H. S. J.; Ruben, M. Spin-crossover in supramolecular iron(II)-2,6-bis(1*H*-pyrazol-1-yl)pyridine complexes: Toward spin-state switchable single-molecule junctions. *ACS Omega* **2022**, *7*, 13654–13666.

[33] Matsumoto, T.; Newton, G. N.; Shiga, T.; Hayami, S.; Matsui, Y.; Okamoto, H.; Kumai, R.; Murakami, Y.; Oshio, H. Programmable spin-state switching in a mixed-valence spin-crossover iron grid. *Nat. Commun.* **2014**, *5*, 3865.

[34] Bousquet, E.; Fava, M.; Romestan, Z.; Gómez-Ortiz, F.; McCabe, E. E.; Romero, A. H. Structural chirality and related properties in periodic inorganic solids: Review and perspectives. *J. Phys.: Condens. Matter* **2025**, *37*, 163004.

[35] Pu, L. Regioselective substitution of BINOL. *Chem. Rev.* **2024**, *124*, 6643–6689.

[36] Fu, G. C. Asymmetric catalysis with "planar-chiral" heterocycles. *Pure Appl. Chem.* **2001**, *73*, 347–349.

[37] Göhler, B.; Hamelbeck, V.; Markus, T. Z.; Kettner, M.; Hanne, G. F.; Vager, Z.; Naaman, R.; Zacharias, H. Spin selectivity in electron transmission through self-assembled monolayers of double-stranded DNA. *Science* **2011**, *331*, 894–897.

[38] Suda, M.; Thathong, Y.; Promarak, V.; Kojima, H.; Nakamura, M.; Shiraogawa, T.; Ehara, M.; Yamamoto, H. M. Light-driven molecular switch for reconfigurable spin filters. *Nat. Commun.* **2019**, *10*, 2455.

[39] Heuer, A. M.; Coste, S. C.; Singh, G.; Mercado, B. Q.; Mayer, J. M. A guide to tris(4-substituted)-triphenylmethyl radicals. *J. Org. Chem.* **2023**, *88*, 9893–9901.

[40] Geraskina, M. R.; Dutton, A. S.; Juetten, M. J.; Wood, S. A.; Winter, A. H. The viologen cation radical pimer: A case of dispersion-driven bonding. *Angew. Chem., Int. Ed.* **2017**, *56*, 9435–9439.

[41] Üngör, Ö.; Shatruk, M. Transition metal complexes with fractionally charged TCNQ radical anions as structural templates for multifunctional molecular conductors. *Polyhedron* **2020**, *177*, 114254.

[42] Frisenda, R.; Gaudenzi, R.; Franco, C.; Mas-Torrent, M.; Rovira, C.; Veciana, J.; Alcon, I.; Bromley, S. T.; Burzurí, E.; van der Zant, H. S. J. Kondo effect in a neutral and stable all organic radical single molecule break junction. *Nano Lett.* **2015**, *15*, 3109–3114.

[43] Hayakawa, R.; Karimi, M. A.; Wolf, J.; Huhn, T.; Zöllner, M. S.; Herrmann, C.; Scheer, E. Large magnetoresistance in single-radical molecular junctions. *Nano Lett.* **2016**, *16*, 4960–4967.

[44] Liu, J. Y.; Zhao, X. T.; Al-Galiby, Q.; Huang, X. Y.; Zheng, J. T.; Li, R. H.; Huang, C. C.; Yang, Y.; Shi, J.; Manrique, D. Z. et al. Radical-enhanced charge transport in single-molecule phenothiazine electrical junctions. *Angew. Chem., Int. Ed.* **2017**, *56*, 13061–13065.

[45] Scott, G. D.; Natelson, D. Kondo resonances in molecular devices. *ACS Nano* **2010**, *4*, 3560–3579.

[46] Selzer, Y.; Allara, D. L. Single-molecule electrical junctions. *Annu. Rev. Phys. Chem.* **2006**, *57*, 593–623.

[47] Parks, J. J.; Champagne, A. R.; Costi, T. A.; Shum, W. W.; Pasupathy, A. N.; Neuscamman, E.; Flores-Torres, S.; Cornaglia, P. S.; Aligia, A. A.; Balseiro, C. A. et al. Mechanical control of spin states in spin-1 molecules and the underscreened Kondo effect. *Science* **2010**, *328*, 1370–1373.

[48] Guo, X.; Zhu, Q. H.; Zhou, L. Y.; Yu, W.; Lu, W. G.; Liang, W. J. Evolution and universality of two-stage Kondo effect in single manganese phthalocyanine molecule transistors. *Nat. Commun.* **2021**, *12*, 1566.

[49] Aligia, A. A. Low-energy physics for an iron phthalocyanine molecule on Au(111). *Phys. Rev. B* **2022**, *105*, 205114.

[50] Liang, W. J.; Shores, M. P.; Bockrath, M.; Long, J. R.; Park, H. Kondo resonance in a single-molecule transistor. *Nature* **2002**, *417*, 725–729.

[51] Xu, J. L.; Zhu, L.; Gao, H.; Li, C. H.; Zhu, M. J.; Jia, Z. Y.; Zhu, X. Y.; Zhao, Y.; Li, S. C.; Wu, F. et al. Ligand non-innocence and single molecular spintronic properties of Ag^{II} dibenzocorrole radical on Ag(111). *Angew. Chem., Int. Ed.* **2021**, *60*, 11702–11706.

[52] Park, J.; Pasupathy, A. N.; Goldsmith, J. I.; Chang, C.; Yaish, Y.; Petta, J. R.; Rinkoski, M.; Sethna, J. P.; Abruña, H. D.; McEuen, P. L. et al. Coulomb blockade and the Kondo effect in single-atom transistors. *Nature* **2002**, *417*, 722–725.

[53] Zyazin, A. S.; van den Berg, J. W. G.; Osorio, E. A.; van der Zant, H. S. J.; Konstantinidis, N. P.; Leijnse, M.; Wegewijs, M. R.; May, F.; Hofstetter, W.; Danieli, C. et al. Electric field controlled magnetic anisotropy in a single molecule. *Nano Lett.* **2010**, *10*, 3307–3311.

[54] Zhao, A. D.; Li, Q. X.; Chen, L.; Xiang, H. J.; Wang, W. H.; Pan, S.; Wang, B.; Xiao, X. D.; Yang, J. L.; Hou, J. G. et al. Controlling the

Kondo effect of an adsorbed magnetic ion through its chemical bonding. *Science* **2005**, *309*, 1542–1544.

[55] Liu, L. W.; Yang, K.; Jiang, Y. H.; Song, B. Q.; Xiao, W. D.; Li, L. F.; Zhou, H. T.; Wang, Y. L.; Du, S. X.; Ouyang, M. et al. Reversible single spin control of individual magnetic molecule by hydrogen atom adsorption. *Sci. Rep.* **2013**, *3*, 1210.

[56] Sarmah, A.; Sarma, M.; Nakajima, T.; Sarma, M.; Hobza, P. Spintronics on demand: Optically tunable Kondo-type phenomena in germanene-azobenzene single-molecule junctions. *J. Phys. Chem. C* **2024**, *128*, 4687–4698.

[57] Mitchell, A. K.; Pedersen, K. G. L.; Hedegård, P.; Paaske, J. Kondo blockade due to quantum interference in single-molecule junctions. *Nat. Commun.* **2017**, *8*, 15210.

[58] Low, J. Z.; Kladnik, G.; Patera, L. L.; Sokolov, S.; Lovat, G.; Kumarasamy, E.; Repp, J.; Campos, L. M.; Cvetko, D.; Morgante, A. et al. The environment-dependent behavior of the Blatter radical at the metal-molecule interface. *Nano Lett.* **2019**, *19*, 2543–2548.

[59] Wagner, S.; Kisslinger, F.; Ballmann, S.; Schramm, F.; Chandrasekar, R.; Bodenstein, T.; Fuhr, O.; Secker, D.; Fink, K.; Ruben, M. et al. Switching of a coupled spin pair in a single-molecule junction. *Nat. Nanotechnol.* **2013**, *8*, 575–579.

[60] Saygun, T.; Bylin, J.; Hammar, H.; Fransson, J. Voltage-induced switching dynamics of a coupled spin pair in a molecular junction. *Nano Lett.* **2016**, *16*, 2824–2829.

[61] Baum, T. Y.; Fernández, S.; Peña, D.; van der Zant, H. S. J. Magnetic fingerprints in an all-organic radical molecular break junction. *Nano Lett.* **2022**, *22*, 8086–8092.

[62] Leiva M, S.; Díaz, S. A.; Nunez, A. S. Origin of the magnetoelectric couplings in the spin dynamics of molecular magnets. *Phys. Rev. B* **2023**, *107*, 094401.

[63] Gaudenzi, R.; de Bruijckere, J.; Reta, D.; Moreira, I. D. P. R.; Rovira, C.; Veciana, J.; van der Zant, H. S. J.; Burzurí, E. Redox-induced gating of the exchange interactions in a single organic diradical. *ACS Nano* **2017**, *11*, 5879–5883.

[64] Molnar, G.; Rat, S.; Salmon, L.; Nicolazzi, W.; Bousseksou, A. Spin crossover nanomaterials: From fundamental concepts to devices. *Adv. Mater.* **2018**, *30*, 1703862.

[65] Bousseksou, A.; Molnár, G.; Salmon, L.; Nicolazzi, W. Molecular spin crossover phenomenon: Recent achievements and prospects. *Chem. Soc. Rev.* **2011**, *40*, 3313–3335.

[66] Johannsen, S.; Ossinger, S.; Grunwald, J.; Herman, A.; Wende, H.; Tuczek, F.; Gruber, M.; Berndt, R. Spin crossover in a cobalt complex on Ag(111). *Angew. Chem., Int. Ed.* **2022**, *61*, e202115892.

[67] Kuang, G. W.; Zhang, Q. S.; Lin, T.; Pang, R.; Shi, X. Q.; Xu, H.; Lin, N. Mechanically-controlled reversible spin crossover of single Fe-porphyrin molecules. *ACS Nano* **2017**, *11*, 6295–6300.

[68] Hao, H.; Zheng, X. H.; Song, L. L.; Wang, R. N.; Zeng, Z. Electrostatic spin crossover in a molecular junction of a single-molecule magnet Fe_2. *Phys. Rev. Lett.* **2012**, *108*, 017202.

[69] Baadji, N.; Piacenza, M.; Tugsuz, T.; Della Sala, F.; Maruccio, G.; Sanvito, S. Electrostatic spin crossover effect in polar magnetic molecules. *Nat. Mater.* **2009**, *8*, 813–817.

[70] Osorio, E. A.; Moth-Poulsen, K.; van der Zant, H. S. J.; Paaske, J.; Hedegård, P.; Flensberg, K.; Bendix, J.; Bjørnholm, T. Electrical manipulation of spin states in a single electrostatically gated transition-metal complex. *Nano Lett.* **2010**, *10*, 105–110.

[71] Harzmann, G. D.; Frisenda, R.; van der Zant, H. S. J.; Mayor, M. Single-molecule spin switch based on voltage-triggered distortion of the coordination sphere. *Angew. Chem., Int. Ed.* **2015**, *54*, 13425–13430.

[72] Yang, C. Y.; Chen, Z. X.; Yu, C. J.; Cao, J. W.; Ke, G. J.; Zhu, W. Y.; Liang, W. X.; Huang, J. X.; Cai, W. Q.; Saha, C. et al. Regulation of quantum spin conversions in a single molecular radical. *Nat. Nanotechnol.* **2024**, *19*, 978–985.

[73] Aravena, D.; Ruiz, E. Coherent transport through spin-crossover single molecules. *J. Am. Chem. Soc.* **2012**, *134*, 777–779.

[74] Gopakumar, T. G.; Matino, F.; Naggert, H.; Bannwarth, A.; Tuczek, F.; Berndt, R. Electron-induced spin crossover of single molecules in a bilayer on gold. *Angew. Chem., Int. Ed.* **2012**, *51*, 6262–6266.

[75] Zeng, J.; Chen, K. Q. Interesting odd-even rules of spin-filtering and magnetoresistance effects in a single-molecule spintronic device. *Carbon* **2016**, *104*, 20–26.

[76] Pei, T.; Thomas, J. O.; Sopp, S.; Tsang, M. Y.; Dotti, N.; Baugh, J.; Chilton, N. F.; Cardona-Serra, S.; Gaita-Ariño, A.; Anderson, H. L. et al. Exchange-induced spin polarization in a single magnetic molecule junction. *Nat. Commun.* **2022**, *13*, 4506.

[77] Cho, W. J.; Cho, Y.; Min, S. K.; Kim, W. Y.; Kim, K. S. Chromium porphyrin arrays as spintronic devices. *J. Am. Chem. Soc.* **2011**, *133*, 9364–9369.

[78] Hao, H.; Zheng, X. H.; Dai, Z. X.; Zeng, Z. Spin-filtering transport and switching effect of MnCu single-molecule magnet. *Appl. Phys. Lett.* **2010**, *96*, 192112.

[79] Safari, M. R.; Matthes, F.; Schneider, C. M.; Ernst, K. H.; Bürgler, D. E. Spin-selective electron transport through single chiral molecules. *Small* **2024**, *20*, 2308233.

[80] Singh, A. K.; Martin, K.; Talamo, M. M., Houssin, A.; Vanthuyne, N.; Avarvari, N.; Tal, O. Single-molecule junctions map the interplay between electrons and chirality. *Nat. Commun.* **2025**, *16*, 1759.

[81] Pal, A. N.; Li, D. Z.; Sarkar, S.; Chakrabarti, S.; Vilan, A.; Kronik, L.; Smogunov, A.; Tal, O. Nonmagnetic single-molecule spin-filter based on quantum interference. *Nat. Commun.* **2019**, *10*, 5565.

[82] Aggarwal, A.; Kaliginedi, V.; Maiti, P. K. Quantum circuit rules for molecular electronic systems: Where are we headed based on the current understanding of quantum interference, thermoelectric, and molecular spintronics phenomena. *Nano Lett.* **2021**, *21*, 8532–8544.

[83] Misiorny, M.; Barnaś, J. Effect of magnetic anisotropy on spin-dependent thermoelectric effects in nanoscopic systems. *Phys. Rev. B* **2015**, *91*, 155426.

[84] Wang, R. Q.; Sheng, L.; Shen, R.; Wang, B. G.; Xing, D. Y. Thermoelectric effect in single-molecule-magnet junctions. *Phys. Rev. Lett.* **2010**, *105*, 057202.

[85] Wu, D.; Cao, X. H.; Chen, S. Z.; Tang, L. M.; Feng, Y. X.; Chen, K. Q.; Zhou, W. X. Pure spin current generated in thermally driven molecular magnetic junctions: A promising mechanism for thermoelectric conversion. *J. Mater. Chem. A* **2019**, *7*, 19037–19044.

[86] Hu, Y. J.; Liu, S. S.; Huang, J.; Li, X. X.; Li, Q. X. Gate-tunable spin Seebeck effect and pure spin current generation in molecular junctions based on bipolar magnetic molecules. *Nano Lett.* **2023**, *23*, 7890–7896.

[87] Zhang, Z. Z.; Jiang, L.; Wang, R. Q.; Wang, B. G.; Xing, D. Y. Thermoelectric-induced spin currents in single-molecule magnet tunnel junctions. *Appl. Phys. Lett.* **2010**, *97*, 242101.

[88] Manaparambil, A.; Weymann, I. Spin Seebeck effect of correlated magnetic molecules. *Sci. Rep.* **2021**, *11*, 9192.

[89] Li, J. W.; Wang, B.; Xu, F. M.; Wei, Y. D.; Wang, J. Spin-dependent Seebeck effects in graphene-based molecular junctions. *Phys. Rev. B* **2016**, *93*, 195426.

[90] Cornaglia, P. S.; Usaj, G.; Balseiro, C. A. Tunable charge and spin Seebeck effects in magnetic molecular junctions. *Phys. Rev. B* **2012**, *86*, 041107.

[91] Raman, K. V.; Kamerbeek, A. M.; Mukherjee, A.; Atodiresei, N.; Sen, T. K.; Lazić, P.; Caciuc, V.; Michel, R.; Stalke, D.; Mandal, S. K. et al. Interface-engineered templates for molecular spin memory devices. *Nature* **2013**, *493*, 509–513.

[92] Pilevarshahri, R.; Rungger, I.; Archer, T.; Sanvito, S.; Shahtahmassebi, N. Spin transport in higher *n*-acene molecules. *Phys. Rev. B* **2011**, *84*, 174437.

[93] Yu, C. J.; Feng, Q. Q.; Li, X. X.; Yang, J. L. Highly interface-dependent spin transport in an Fe-Mn(DBTAA)-Fe single molecule spintronic device. *Nanoscale* **2022**, *14*, 15799–15803.

[94] Li, J. J.; Bai, M. L.; Chen, Z. B.; Zhou, X. S.; Shi, Z.; Zhang, M.; Ding, S. Y.; Hou, S. M.; Schwarzacher, W.; Nichols, R. J. et al.

Giant single-molecule anisotropic magnetoresistance at room temperature. *J. Am. Chem. Soc.* **2015**, *137*, 5923–5929.
[95] Aragonès, A. C.; Aravena, D.; Valverde-Muñoz, F. J.; Real, J. A.; Sanz, F.; Díez-Pérez, I.; Ruiz, E. Metal-controlled magnetoresistance at room temperature in single-molecule devices. *J. Am. Chem. Soc.* **2017**, *139*, 5768–5778.
[96] Aragonès, A. C.; Aravena, D.; Cerdá, J. I.; Acís-Castillo, Z.; Li, H. P.; Real, J. A.; Sanz, F.; Hihath, J.; Ruiz, E.; Díez-Pérez, I. Large conductance switching in a single-molecule device through room temperature spin-dependent transport. *Nano Lett.* **2016**, *16*, 218–226.
[97] Mitra, G.; Low, J. Z.; Wei, S. J.; Francisco, K. R.; Deffner, M.; Herrmann, C.; Campos, L. M.; Scheer, E. Interplay between magnetoresistance and Kondo resonance in radical single-molecule junctions. *Nano Lett.* **2022**, *22*, 5773–5779.
[98] Emberly, E. G.; Kirczenow, G. Molecular spintronics: Spin-dependent electron transport in molecular wires. *Chem. Phys.* **2002**, *281*, 311–324.
[99] Shiraishi, M.; Ikoma, T. Molecular spintronics. *Phys. E: Low-dimens. Syst. Nanostructur.* **2011**, *43*, 1295–1317.
[100] Pati, R.; Senapati, L.; Ajayan, P. M.; Nayak, S. K. First-principles calculations of spin-polarized electron transport in a molecular wire: Molecular spin valve. *Phys. Rev. B* **2003**, *68*, 100407.
[101] Schmaus, S.; Bagrets, A.; Nahas, Y.; Yamada, T. K.; Bork, A.; Bowen, M.; Beaurepaire, E.; Evers, F.; Wulfhekel, W. Giant magnetoresistance through a single molecule. *Nat. Nanotechnol.* **2011**, *6*, 185–189.
[102] Zu, F. X.; Liu, Z. L.; Yao, K. L.; Gao, G. Y.; Fu, H. H.; Zhu, S. C.; Ni, Y.; Peng, L. Nearly perfect spin filter, spin valve and negative differential resistance effects in a Fe_4-based single-molecule junction. *Sci. Rep.* **2014**, *4*, 4838.
[103] Rizzini, A. L.; Krull, C.; Balashov, T.; Kavich, J. J.; Mugarza, A.; Miedema, P. S.; Thakur, P. K.; Sessi, V.; Klyatskaya, S.; Ruben, M. et al. Coupling single molecule magnets to ferromagnetic substrates. *Phys. Rev. Lett.* **2011**, *107*, 177205.
[104] Yang, C.; Li, Y. W.; Zhou, S. Y.; Guo, Y. L.; Jia, C. C.; Liu, Z. R.; Houk, K. N.; Dubi, Y.; Guo, X. F. Real-time monitoring of reaction stereochemistry through single-molecule observations of chirality-induced spin selectivity. *Nat. Chem.* **2023**, *15*, 972–979.
[105] Ke, G. J.; Duan, C. H.; Huang, F.; Guo, X. F. Electrical and spin switches in single-molecule junctions. *InfoMat* **2020**, *2*, 92–112.
[106] Yang, K.; Chen, H.; Pope, T.; Hu, Y. B.; Liu, L. W.; Wang, D. F.; Tao, L.; Xiao, W. D.; Fei, X. M.; Zhang, Y. Y. et al. Tunable giant magnetoresistance in a single-molecule junction. *Nat. Commun.* **2019**, *10*, 3599.
[107] Xing, Y. Q.; Chen, H.; Hu, B.; Ye, Y. H.; Hofer, W. A.; Gao, H. J. Reversible switching of Kondo resonance in a single-molecule junction. *Nano Res.* **2022**, *15*, 1466–1471.
[108] Ormaza, M.; Abufager, P.; Verlhac, B.; Bachellier, N.; Bocquet, M. L.; Lorente, N.; Limot, L. Controlled spin switching in a metallocene molecular junction. *Nat. Commun.* **2017**, *8*, 1974.
[109] Wäckerlin, C.; Chylarecka, D.; Kleibert, A.; Müller, K.; Iacovita, C.; Nolting, F.; Jung, T. A.; Ballav, N. Controlling spins in adsorbed molecules by a chemical switch. *Nat. Commun.* **2010**, *1*, 61.
[110] Li, J.; Wu, Q. Q.; Xu, W.; Wang, H. C.; Zhang, H. W.; Chen, Y. R.; Tang, Y. X.; Hou, S. J.; Lambert, C. J.; Hong, W. J. Room-temperature single-molecule conductance switch via confined coordination-induced spin-state manipulation. *CCS Chem.* **2022**, *4*, 1357–1365.
[111] Komeda, T.; Isshiki, H.; Liu, J.; Zhang, Y. F.; Lorente, N.; Katoh, K.; Breedlove, B. K.; Yamashita, M. Observation and electric current control of a local spin in a single-molecule magnet. *Nat. Commun.* **2011**, *2*, 217.
[112] Köbke, A.; Gutzeit, F.; Röhricht, F.; Schlimm, A.; Grunwald, J.; Tuczek, F.; Studniarek, M.; Longo, D.; Choueikani, F.; Otero, E. et al. Reversible coordination-induced spin-state switching in complexes on metal surfaces. *Nat. Nanotechnol.* **2020**, *15*, 18–21.
[113] Bandyopadhyay, S.; Cahay, M. Electron spin for classical information processing: A brief survey of spin-based logic devices, gates and circuits. *Nanotechnology* **2009**, *20*, 412001.
[114] Kovarik, S.; Schlitz, R.; Vishwakarma, A.; Ruckert, D.; Gambardella, P.; Stepanow, S. Spin torque-driven electron paramagnetic resonance of a single spin in a pentacene molecule. *Science* **2024**, *384*, 1368–1373.
[115] Chiesa, A.; Privitera, A.; Macaluso, E.; Mannini, M.; Bittl, R.; Naaman, R.; Wasielewski, M. R.; Sessoli, R.; Carretta, S. Chirality-induced spin selectivity: An enabling technology for quantum applications. *Adv. Mater.* **2023**, *35*, 2300472.
[116] Sellies, L.; Spachtholz, R.; Bleher, S.; Eckrich, J.; Scheuerer, P.; Repp, J. Single-molecule electron spin resonance by means of atomic force microscopy. *Nature* **2023**, *624*, 64–68.
[117] Willke, P.; Bilgeri, T.; Zhang, X.; Wang, Y.; Wolf, C.; Aubin, H.; Heinrich, A.; Choi, T. Coherent spin control of single molecules on a surface. *ACS Nano* **2021**, *15*, 17959–17965.
[118] Liu, M.; Zhu, J. Y.; Zhao, G. H.; Li, Y. X.; Yang, Y. P.; Gao, K. M.; Wu, K. F. Coherent manipulation of photochemical spin-triplet formation in quantum dot-molecule hybrids. *Nat. Mater.* **2025**, *24*, 260–267.
[119] Gaita-Ariño, A.; Luis, F.; Hill, S.; Coronado, E. Molecular spins for quantum computation. *Nat. Chem.* **2019**, *11*, 301–309.
[120] Fu, P. X.; Zhou, S.; Liu, Z.; Wu, C. H.; Fang, Y. H.; Wu, Z. R.; Tao, X. Q.; Yuan, J. Y.; Wang, Y. X.; Gao, S. et al. Multiprocessing quantum computing through hyperfine couplings in endohedral fullerene derivatives. *Angew. Chem., Int. Ed.* **2022**, *61*, e202212939.
[121] Hu, Z. Q.; Dong, B. W.; Liu, Z.; Liu, J. J.; Su, J.; Yu, C. C.; Xiong, J.; Shi, D. E.; Wang, Y. Y.; Wang, B. W. et al. Endohedral metallofullerene as molecular high spin qubit: Diverse Rabi cycles in $Gd_2@C_{79}N$. *J. Am. Chem. Soc.* **2018**, *140*, 1123–1130.
[122] Moreno-Pineda, E.; Godfrin, C.; Balestro, F.; Wernsdorfer, W.; Ruben, M. Molecular spin qudits for quantum algorithms. *Chem. Soc. Rev.* **2018**, *47*, 501–513.